CHALMERS
UNIVERSITY OF TECHNOLOGY

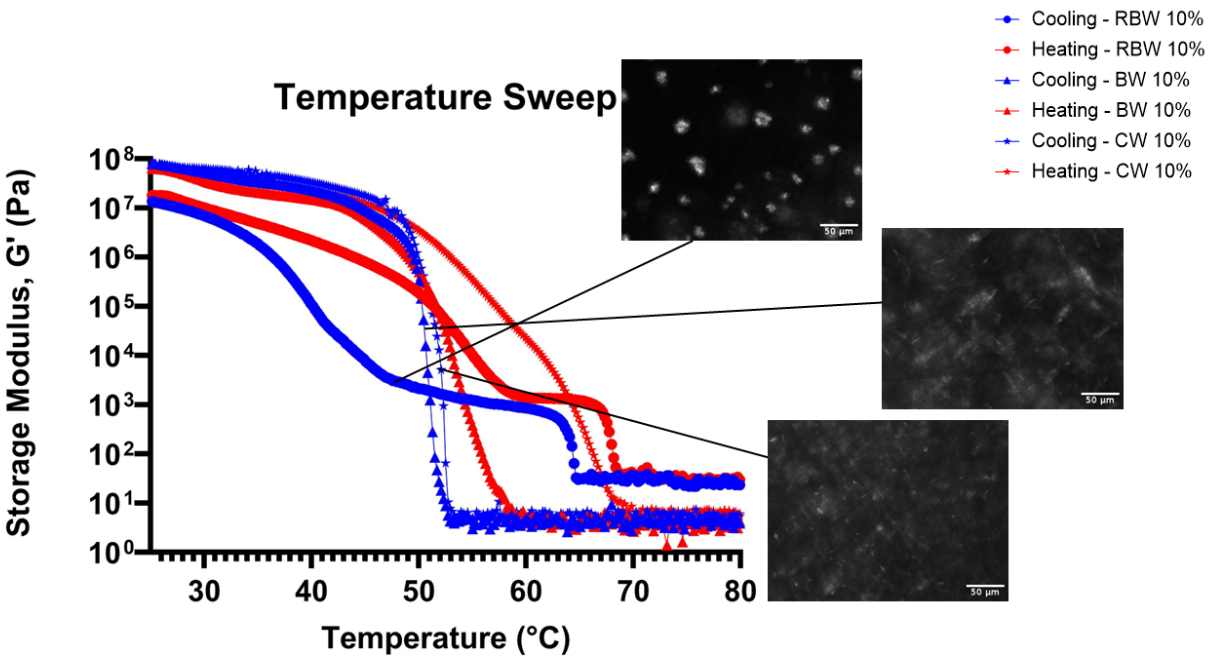

Developments of oleogels for plant-based meat analogues

Master's thesis in Biotechnology

Samuel Lindroth

DEPARTMENT OF CHEMISTRY

CHALMERS UNIVERSITY OF TECHNOLOGY
Gothenburg, Sweden 2024
www.chalmers.se

Master's thesis 2024

Developments of oleogels for plant-based meat analogues

Samuel Lindroth

CHALMERS
UNIVERSITY OF TECHNOLOGY

Department of Chemistry
Division of Applied Chemstry
Chalmers University of Technology
Gothenburg, Sweden 2024

Developments of oleogels for plant-based meat analogues
Samuel Lindroth

Supervisors: Johanna Andersson and Astrid Ahlinder,
Research Institute of Sweden

Examiner: Anna Ström, Applied Chemistry, Department of Chemistry and Chemical Engineering, Chalmers University of Technology

Master's Thesis 2024
Department of Chemistry and Chemical Engineering
Division of Applied Chemistry
Chalmers University of Technology
SE-412 96 Gothenburg
Telephone +46 31 772 1000

Cover: Temperature sweeps of three oleogels with natural wax and rapeseed oil, with accompanying rheomicroscopy images.

Typeset in LaTeX
Printed by Chalmers Reproservice
Gothenburg, Sweden 2024

Developments of oleogels for plant-based meat analogues
Samuel Lindroth Department of Chemistry
Chalmers University of Technology

Abstract

The escalating concerns surrounding meat consumption and the detrimental effects of saturated fats on both human health and the environment underscore the urgent need for sustainable dietary alternatives. In response to these challenges, oleogels, structured lipid systems composed of liquid oil and a structuring agent, have emerged as a promising solution. Mimicking the structural properties of animal fats, oleogels offer a viable component for formulating plant-based meat analogues, providing desirable texture and mouthfeel while eliminating the health risks associated with saturated fats. Hence, the aims for this thesis were firstly to successfully formulate oleogels using natural waxes and rapeseed oil and secondly to develop a methodology to evaluate the rheological and thermodynamical behaviour of the gels using rheomicroscopy and differential scanning calorimetry (DSC).

Oleogels were successfully formulated using direct dispersion with the natural waxes, rice bran wax (RBW), beeswax (BW), candelilla wax (CW) and carnauba wax (CBW) as oleogelators and rapeseed oil as the liquid phase. Oleogels with 10% w/w RBW, BW and CW was further evaluated using rheomicroscopy to investigate the microstructural organisation of the gels, providing complementary insights into the relationship between crystal morphology and rheological behavior. DSC was utilised to also examine the thermal behavior and phase transitions of oleogels, enabling a comprehensive understanding of their crystallization kinetics and polymorphic behavior.

The chemical composition of the waxes and how they interacted with the oil phase was determined to be crucial in the understanding of the gelation process and viscoelastic properties of the gels. The rheological analysis and microscopic images revealed distinct differences in the viscoelastic properties and structure. Gels containing CW and BW exhibited higher stiffness and gel strength compared to RBW oleogels, attributed to the formation of dense, organized crystal networks of smaller needle-like crystals. RBW gels were stable at higher temperatures than BW and CW, but formed more randomly organised structures from roundly, dendritically shaped crystals. Additionally, DSC confirmed unique thermal behaviours for each wax, with CW requiring the least energy for crystallisation and melting, followed by BW and RBW. These findings highlight the influence of wax type on the structural and thermal properties of oleogels, underscoring the importance of wax selection in optimizing oleogel formulations for various applications.

Keywords: oleogel, oleogelator, rapeseed oil, natural waxes, meat analogues, rheomicroscopy, crystallisation, differential scanning calorimetry.

Acknowledgements

I would like to express my sincere gratitude and appreciation to my supervisors Johanna Andersson and Astrid Ahlinder at RISE, whose guidance, support, and expertise have been invaluable throughout the journey of completing this master's thesis. Their insightful feedback, encouragement, and patience have greatly contributed to the development and completion of this work. I am especially grateful to Astrid for dedicating her time and expertise in the laboratory to mentor and instruct me in the utilisation of rheometry and differential scanning calorimetry techniques. Meanwhile, Johanna always ensured the project stayed aligned with our primary goals and continuously provided valuable insights on how to keep moving forward, which made them the perfect team to guide me through this project.

I am also thankful to my examiner, Anna Ström, for taking the time to review and evaluate this thesis. Her constructive criticism and valuable suggestions have undoubtedly enhanced the quality of this research. The same goes for my opponent, Kajsa Grönqvist, whose thoughtful feedback and insightful comments have contributed to improving this work.

Furthermore, I extend my heartfelt thanks to my colleagues at RISE who have provided support, encouragement, and assistance along the way. Also a huge thanks to the four other master's students working at RISE, as their camaraderie and shared experiences have made this endeavour more enjoyable and rewarding. I want to especially thank a master's student from Gent University, Astrid Hemeryck, who also worked on the FOMA project, as she contributed to many brain-storming sessions and ideas. Her work also complimented my master's thesis by producing light microscopy images of the oloegels, enabling me to compare my work with hers.

Last, but not least, I am deeply grateful to my family and friends for their unwavering love, encouragement, and understanding which has motivated me greatly throughout this academic journey.

Samuel Lindroth, Gothenburg, June 2024

List of Acronyms

Below is the list of acronyms that have been used throughout this thesis listed in alphabetical order:

BW	Beeswax
CW	Candelilla wax
CBW	Carnauba wax
DSC	Differential Scanning Calorimetry
FOMA	Fats and Oils in Meat Analogues
HDL	High-Density Lipoprotein
HMWOG	High molecular weight oleogelator
LDL	Low-Density Lipoprotein
LMWOG	Low molecular weight oleogelator
LVR	Linear viscoelastic region
MUFA	Monounusaturated Fatty Acid
PBMA	Plant-Based Meat Analogue
PUFA	Polyunsaturated Fatty Acid
RBW	Rice bran wax
RSO	Rapeseed oil
RISE	Research Institute of Sweden
TAG	Triacylglyceride

Contents

List of Acronyms **ix**

List of Figures **xiii**

List of Tables **xv**

1 Introduction **1**
1.1 Purpose and objectives . . . 1
1.2 Limitations . . . 2

2 Theory **3**
2.1 Health and environmental aspects of fats . . . 3
2.2 Oleogels . . . 4
2.2.1 Vegetable oils . . . 5
2.2.1.1 Rapeseed oil . . . 6
2.2.2 Oleogelators . . . 6
2.2.2.1 Waxes . . . 7
2.2.2.2 Rice bran wax . . . 7
2.2.2.3 Beeswax . . . 8
2.2.2.4 Candelilla wax . . . 8
2.2.2.5 Carnauba wax . . . 8
2.3 Formulating oleogels . . . 8
2.3.1 Direct dispersion . . . 9
2.4 Rheology . . . 9
2.4.1 Storage and loss modulus . . . 9
2.4.2 Rheometry . . . 11
2.4.3 Amplitude and frequency sweep . . . 11
2.4.4 Oscillation and rotation . . . 12
2.5 Differential scanning calorimetry . . . 12

3 Methods **15**
3.1 Materials . . . 15
3.2 Oleogel preparation . . . 15
3.2.1 Wax-based oleogels . . . 15
3.3 Rheological measurements . . . 16
3.3.1 Amplitude sweep . . . 17
3.3.2 Frequency and temperature sweeps . . . 17

3.3.3 Rheomicroscopy 18
3.4 Differential scanning calorimetry 18

4 Results and discussion **19**
4.1 Oleogel preparation 19
4.2 Rheological measurements 20
4.2.1 Amplitude sweeps and frequency sweeps 20
4.2.2 Temperature sweeps 22
4.2.3 Rheomicroscopy 24
4.3 Thermal characterization 27
4.3.1 Rapeseed oil 27
4.3.2 Waxes 28
4.3.3 Oleogels 29
4.4 Methodological evaluation 32
4.4.1 Choice of oleogels 32
4.4.2 Rheology 33
4.4.3 DSC 34

5 Conclusion and prospects **37**

Bibliography **39**

A Appendix 1 **I**
A.1 Temperature sweeps I

List of Figures

2.1 Chemical structure of rapeseed oil (RSO), showing the glycerol backbone attached to the three main fatty acid chains of RSO, oleic acid, linoelic acid and linolenic acid. (Created in ChemDoodle). 6

2.2 Vector diagram illustrating the relationship between storage modulus *G'* (elastic shear), *G"*(viscous shear) and complex shear modulus *G**, including the phase shift angle δ. The y-axis represents the viscous portion, while the x-axis represents the elastic portion. (Made in Google Drawings). 10

3.1 Images of the HR30, hybrid rheomicroscope, used for the rheological and microscopic measurements. 17

4.1 Visual appearance of the oleogels with rice bran wax (RBW), beeswax (BW), carnauba wax (CBW) and candelilla wax (CW) at 10% and 5% w/w wax. 19

4.2 Overview of constructed olegels with 10% w/w of rice bran wax (RBW10), beeswax (BW10) and candelilla wax (CW10). 20

4.3 Frequency sweeps of the oleogels RBW10, BW10 and CW10. Both sweeps are at 25 °C. a) Frequency sweep I, shown at the top, refers to the sweep conducted directly after placing the oleogel on the plate. b) Frequency sweep II, in the bottom, occurs after exposing the gels to one heating and one cooling ramp. 21

4.4 Temperature sweeps, from 80 °C to 25 °C and back, of the oleogels RBW10, BW10 and CW10. Cooling ramps are shown in blue and heating ramps in red, with different representative symbols for each oleogel. 22

4.5 Temperature sweeps of the oleogels RBW10, BW10 and CW10 showing the response of the phase angle during cooling and heating ramp separately. 23

4.6 Isolated temperature sweep of RBW10 with images from the rheomicroscope at two approximate points during the cooling and heating ramps. 24

4.7 Isolated temperature sweep of BW10 with images from the rheomicroscope at two approximate points during the cooling and heating ramps. 25

4.8 Isolated temperature sweep of CW10 with images from the rheomicroscope at two approximate points during the cooling and heating ramps. 25
4.9 Snapshot images from the cooling ramps of the temperature sweep, at the time points when crystallisation is visible, a) RBW10, b) BW10 and c) CW10. 26
4.10 Polarised light microscopy images of a) RBW10, b) BW10 and c) CW10. 26
4.11 DSC of rapeseed oil (RSO). 27
4.12 DSC of the natural waxes. 28
4.13 DSC of the oleogels with 10% w/w of rice bran wax (RBW10), beeswax (BW10) and candelilla wax (CW10). 29
4.14 DSC showing the cooling ramp, using both 2 K/min and 10 K/min temperature change rate, of the oleogels with 10% w/w of rice bran wax (RBW10), beeswax (BW10) and candelilla wax (CW10) 30
4.15 DSC showing the heating ramp, using both 2 K/min and 10 K/min temperature change rate, of the oleogels with 10% w/w of rice bran wax (RBW10), beeswax (BW10) and candelilla wax (CW10) 31

A.1 Isolated temperature sweep of RBW10 with error bars showing the range intervals of the three replicates. I
A.2 Isolated temperature sweep of BW10 with error bars showing the range intervals of the three replicates. I
A.3 Isolated temperature sweep of CW10 with error bars showing the range intervals of the three replicates. II

List of Tables

3.1 Ranges of melting temperatures for the waxes used in the making of the oleogels according to the manufacturers TER Chemicals (Hamburg, Germany). 16
3.2 Overview of constructed oleogels displaying the sample names, the used gelator and the weight percentage of the gelator. 16

4.1 Calculated mean and standard deviation values for the three replicates of rapeseed oil (RSO) from DSC. 27
4.2 Calculated mean and standard deviation values for the three replicates of the natural waxes in neat form, from DSC. 29
4.3 Calculated mean and standard deviation values for the three replicates of the oleolges with rice bran wax (RBW10), beeswax (BW10) and candelilla wax(CW10), respectively, from DSC. 29

1
Introduction

Fats, particularly saturated and trans fats commonly found in animal products, have long been associated with increased risks of chronic diseases like heart disease and stroke [1]. These detrimental health impacts, coupled with the significant environmental footprint of animal agriculture, call for plant-based alternatives that can offer comparable sensory experiences without adverse consequences. Hence, the global trend towards healthier and more sustainable diets demands the need for innovative approaches to food production. However, replicating the complex textural and organoleptic qualities imparted by animal fats in plant-based products remains a major obstacle. Oleogels pose as a promising solution, as they allow for the structuring of healthy plant-based oils into solid-like materials [2]. This unique characteristic of oleogels enables them to mimic the textural and functional properties of animal fats in plant-based meat alternatives. Additionally, oleogels can be formulated with carefully selected ingredients, offering superior nutritional profiles, characterised by elevated levels of unsaturated fats beneficial for cardiovascular health, compared to traditional meat products [2]. By addressing both health and environmental concerns, oleogels hold the potential to produce plant-based meat analogues (PBMAs) that are not only healthier and more sustainable, but also highly desirable in terms of taste and texture in comparison to meat substitutes available today. The purpose of implementing oleogels is therefore to enhance the overall quality of plant-based alternatives, making them healthier and more palatable to consumers to improve the liking and acceptance of meat analogues, while addressing the growing demand for sustainable and vegan protein sources.

1.1 Purpose and objectives

This project aimed to investigate the rheological and thermodynamic properties of wax-based oleogels with the intention to be used in PBMAs. The rheological behaviour and microstructure of these oleogels were analysed, as well as their thermodynamic behaviour, focusing on their heat flow characteristics and phase transitions. Specifically, the focus was to develop oleogel formulations that enhance the texture of PBMAs, using rapeseed oil as the liquid oil phase together with different natural waxes as oleogelators, to create stabilising networks that entrap the oil. As this project was part of a larger project at RISE, called "Fats and oils in meat analogues" (FOMA), the intended outcome was to provide oleogel formulations that, when co-extruded with soy protein isolate and pea fibre, result in PBMAs with superior sensory attributes and nutritional profiles. However, this master's thesis was

mainly concerned with the development and characterization of the rheological and thermal properties of the oleogels using rheometry, rheomicroscopy and differential scanning calorimetry (DSC).

One of the main objectives of this thesis was to implement rheomicroscopy, which offers a unique advantage in the characterisation of oleogels, by providing real-time visualisation of their microstructural changes under various shear and temperature conditions. The crystals forming the network were at a length scale ranging from approximately 10-100 µm, which suited rheomicroscopy well. The main focus area was to visualise the melting and crystallisation of the oleogels during heating and cooling ramps. By implementing rheomicroscopy, the method allowed for observing the gel networks, identifying their phase transitions and assessing their structural stability during different temperature and strain conditions. Therefore, an effort was put into developing a robust methodology for rheomicroscopy to enable accurate interpretation of the rheological behaviour of oleogels, facilitating a deeper understanding of their structure-property relationships.

To complement the rheological measurements, utilizing DSC to measure heat flow during the phase transitions, provided a comprehensive understanding of the thermal properties of the oleogel. DSC offered insights into the thermal behaviour of oleogels by quantifying heat flow changes during phase transitions such as melting and crystallization. This complementary technique enhanced the rheological assessments by elucidating the underlying thermal phenomena driving structural changes in the oleogel matrices.

1.2 Limitations

For the preparation of oleogels, this thesis did not include any indirect construction methods, such as solvent exchange or biphasic emulsions, nor did it deal with oleogelators of high molecular weight such as polymers. The constructed oleogels used in this thesis did not consist of more than two components. Neither was a particular focus set on evaluating many different concentrations of oleogelators, as this too would have contributed to many more experiments needing to be done, which would not have fitted within the time frame of the thesis work.

Extrusion trials was not included, even though important characteristics for extrusion, such as heat stability, shear strain and shear stress was considered when evaluating the oleogels, but they were not optimized for extrusion.

2

Theory

2.1 Health and environmental aspects of fats

The harmful effects of trans and saturated fatty acids on human health, and ways to lessen their impact, have been a topic of debate for many years. While dietary fats are essential for various bodily functions, specific types can significantly impact our risk of chronic diseases. Previous studies have shown that a diet high in saturated and trans fatty acids demonstrates correlations with increased susceptibility to various diseases, including coronary heart disease, type II diabetes, obesity, stroke, metabolic syndrome, and other disorders related to the levels of cholesterol [1]. Understanding this intricate relationship between fats and health is crucial when developing innovative alternatives to meat-based products. On the one hand, saturated fats found predominantly in animal sources like red meat and dairy, have raised concerns due to their potential to increase the low-density lipoprotein (LDL) cholesterol levels in the bloodstream [3]. This rise in LDL cholesterol contributes to plaque buildup in arteries, a major risk factor for heart disease and stroke. Additionally, trans fats, artificially created through hydrogenation and once widely used in processed foods, further exacerbate cardiovascular risks by not only raising LDL but also lowering high-density lipoprotein (HDL) cholesterol [3].

Unsaturated fats, possessing at least one double bond in their carbon chain, offer a healthier alternative. These fats can be further categorized into monounsaturated fatty acids (MUFAs) and polyunsaturated fatty acids (PUFAs). MUFAs, abundant in many vegetable products such as rapeseed oil, olive oil, avocados, and nuts, can positively impact health by lowering LDL cholesterol while maintaining HDL levels [3]. They are also associated with improved blood sugar control and reduced inflammation. PUFAs can be further divided into omega-3 and omega-6 fatty acids, two of the most important essential fatty acids, meaning that they cannot be synthesised by the body, so they must be obtained from the diet. These fatty acids play critical roles in various physiological processes, such as maintaining cell membrane integrity, supporting brain function, regulating inflammation, and contributing to the structure and function of the nervous system. Good dietary sources of omega-3 fatty acids include fatty fish, flaxseeds, chia seeds, and walnuts, while omega-6 fatty acids are commonly found in vegetable oils, nuts, and seeds.[3].

Meat production and consumption contribute significantly to environmental challenges, such as deforestation, greenhouse gas emissions, water pollution, and biodi-

versity loss, exacerbating habitat destruction, climate change, and water scarcity[4]. To address these concerns, there is a growing interest in transitioning towards plant-based alternatives, which potentially could require fewer resources and emit less amount of greenhouse gases [4]. PBMAs offer a sustainable alternative, especially if they closely resemble conventional meat in taste and texture. Promoting the adoption of plant-based diets and incorporating an innovative technology like oleogels to enhance the organoleptic properties of PBMAs, is a potential strategy to mitigate the environmental impact of meat production and consumption while meeting consumer preferences for taste and nutrition.

2.2 Oleogels

The concerning health effects of saturated and trans fats, along with ethical and environmental considerations related to animal agriculture, have fueled the burgeoning market for plant-based meat alternatives. These alternatives aim to mimic the sensory experience, including texture, taste, and aroma, of traditional meat while offering a healthier and more sustainable dietary option. However, replicating the fat content and texture of meat solely with plant-based ingredients poses a significant challenge. Directly incorporating oil into PBMAs during high-moisture extrusion proves to be problematic for the final product as the oil would not bind effectively within the protein matrix [5]. Firstly, oil disrupts the protein-protein interactions crucial for forming the fibrous network that mimics meat texture, and as oil acts as a lubricant, it reduces the internal friction necessary for protein alignment and fibre formation. Secondly, oil distribution within the protein matrix is often uneven, leading to a greasy mouthfeel and potentially compromising the structural integrity of the product [5]. One possible mitigation strategy to overcome the extrusion challenges is the rising interest in oleogels, which comes with the potential to utilise healthier oils, rich in unsaturated fats, to improve the nutritional profile and organoleptic properties of plant-based alternatives [2].

The definition of a gel is a material with a three-dimensional network structure that traps a liquid phase. In a conventional gel, this network is formed by hydrophilic polymers that disperse throughout a liquid, often water. The entangled polymer chains create a physical barrier that restricts the flow of the liquid, resulting in the characteristic gel-like consistency [6]. In contrast, oleogels possess a network formed by oleogelators, specific molecules that self-assemble within a non-polar liquid, typically oil. These oleogelator networks mimic the function of polymers in gels, trapping the oil phase and preventing its free flow. This distinction in network formation results in oleogels being hydrophobic, repelling water, while traditional gels are hydrophilic. Despite these differences, both gels and oleogels exhibit the unique property of maintaining a solid-like structure while incorporating a significant amount of liquid. Oleogels in turn are as mentioned gels in which the continuous liquid phase consists of an oil, or a mixture of oils, being retained by a network created from an oleogelator [2]. The network generates lipid systems that provide a gel-like consistency of fats. Gels made with a majority of water as the continuous phase, called hydrogels, are well-known and commonly used today, but

the interest in oleogels has risen, due to that they can play a vital role in adapting the texture and mouthfeel of food products. Traditionally, animal-based hard fats or hydrogenated plant-based fats are utilised for their firmness and texture, but with the development of oleogels, formulations can be made with healthier oils, such as those rich in unsaturated fats, and can contribute to a better lipid profile and overall nutritional profile [2]. Therefore, on the contrary to animal fats, oleogels can be designed to be rich in both MUFAs and PUFAs, while still maintaining a firm and solid structure. One previous study in particular shows the incorporation of olgeogels to improve the nutritional value of pastries using rapeseed oil and sunflower wax. The results showed a decrease of saturated fatty acids from 29%-47% to 7%–13% and an increase of polyunsaturated fatty acids of at least 22% in oleogel-based cookies [7]. There are various options available for oils and oleogelators to be used in the food sector, and the nature of both the gelling solvent and the gelling agent greatly influences the textural, thermal and rheological properties of the constructed oleogel [8]. However, during extrusion of food products, there are problematic aspects of implementing oleogels. Firstly, the oleogel must exhibit high thermal stability and shear resistance to withstand the high temperatures and pressures encountered during extrusion, to ensure that the oleogelator network remains intact and effectively entraps the oil within the product. Secondly, compatibility with other ingredients, especially the protein matrix, is crucial. Incompatibility can lead to undesirable effects like phase separation or disruption of the protein network, negatively impacting the final texture. Lastly, processability is essential as the oleogel should be readily incorporated into existing extrusion procedures without significant modifications. Ideally, it should be easily dispersible in the oil phase at a suitable temperature. Addressing these factors will be critical for the successful utilization of oleogels in extruded food applications. Further aspects that are crucial to take into account are food grade, availability, low costs and sensory equivalence [2].

2.2.1 Vegetable oils

Vegetable oils consist primarily of triacylglycerides (TAGs), where each molecule is composed of a glycerol backbone, connected to three fatty acid chains through ester linkages. These fatty acids vary in length and saturation, influencing the physical properties of the oil, such as viscosity, melting point, and stability. Unsaturated fatty acids, prevalent in vegetable oils, contribute to fluidity and lower melting points, while saturated fatty acids enhance stability and resistance to oxidation [2]. In the context of oleogels, the most influential aspect for the choice of oil within the formulations is the chemical structure, mainly the amount of unsaturated fatty acids and fatty acid chain length. Oils abundant in unsaturated fatty acids foster flexible and fluid gel networks, creating softer textures and lower melting points, while oils with higher proportions of saturated fatty acids yield stiffer and more stable gels, suited for firmer textures and increased thermal stability [2]. Other important characteristics of oil which also have a great effect on crystallisation behaviour and gelation kinetics, are the polarity and viscosity of the oil [9]. The polarity of oil dictates its compatibility with other components and influences the formation of stable networks in oleogels. Oils with higher polarity tend to interact more readily with

structuring agents, facilitating the formation of gels with desirable properties such as texture and stability [10]. Conversely, viscosity plays a crucial role in determining the flow behaviour of oil within the gel network, impacting its mechanical properties and shelf stability. Oils with higher viscosity exhibit slower diffusion rates. While this does not directly translate to denser networks, it can influence the gelation process of some oleogels. Slower diffusion may allow the oleogelator molecules more time to interact and form a more stable network, potentially leading to enhanced stability over time[11]. Examples of vegetable oils that are widely used in food today are rapeseed oil (RSO), sunflower oil and olive oil [2].

2.2.1.1 Rapeseed oil

RSO is typically extracted from the seeds of the rapeseed plant through a process called cold pressing or solvent extraction. In cold pressing, the seeds are mechanically pressed to release the oil without the use of heat or chemicals, preserving the natural flavour and nutritional qualities of the oil. Rapeseed plants contribute significantly to southern Sweden's agricultural landscape, hence being a highly regional resource. In regards to the chemical structure of RSO, it consists of triglycerides with a blend of saturated, monounsaturated, and polyunsaturated fatty acid chains. Among these, oleic acid (C18:1), linoleic acid (C18:2), and linolenic acid (C18:3) dominate, each contributing distinct properties to the oil [12]. Being rich in unsaturated fats, rapeseed oil can help reduce levels of harmful cholesterol and lower the risk of cardiovascular diseases when consumed as part of a balanced diet [1]. The chemical structure of RSO is shown in figure 2.1, displaying the TAG with the three most common fatty acids.

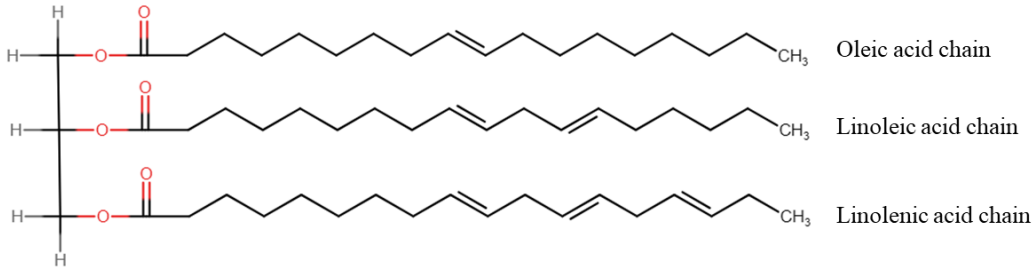

Figure 2.1: Chemical structure of rapeseed oil (RSO), showing the glycerol backbone attached to the three main fatty acid chains of RSO, oleic acid, linoelic acid and linolenic acid. (Created in ChemDoodle).

2.2.2 Oleogelators

There are two main classes of gelators in regards to oleogels, called low molecular weight oleogelators (LMWOGs) and high molecular weight oleogelators (HMWOGs) [2]. LMWOGs are capable of self-assembling into a robust crystal network, which is essential for stabilizing the resulting oleogel. The formation of this network, governed by physical interactions such as Van der Waals forces, hydrophobic interactions, and hydrogen bonding, is greatly influenced by temperature and shear forces.

Within this category of oleogelators are various compounds including waxes, fatty acids, alcohols, mono-acylglycerols, ceramides, and β-sitosterol/γ-oryzanol which are found are natural compounds in various plant sources. HMWOGs on the contrary are capable of trapping oil by creating a three-dimensional network through chemical interactions such as hydrogen bonding and dipole-dipole moments [2]. These compounds are often proteins and polysaccharides, such as the polysaccharide ethylcellulose. Oleogels made with polymeric oleogelators exhibit viscoelastic properties that are significantly affected by the molecular weight, conformation, and concentration of the polymers [2].

2.2.2.1 Waxes

Natural waxes, a diverse group of complex esters, alcohols, and hydrocarbons, have emerged as promising candidates for oleogel applications due to their inherent crystalline gelation properties [13]. These waxes, derived from plants, animals, or insects, offer several advantages over traditional synthetic alternatives. Firstly, their natural origin often translates to biodegradability and non-toxicity, aligning with the growing demand for sustainable materials. Secondly, the intricate chemical structures of natural waxes can lead to the formation of diverse gel networks with unique properties. By tailoring the type and concentration of the wax, factors like gel strength, viscosity, and thermal stability can be controlled, enabling the design of oleogels suited for specific applications [13].

The mechanism for gelation in regards to waxes as oleogelators, comes from the structuring of n-alkanes or wax esters into microcrystalline platelets, which in turn, upon aggregation, can form a complex three-dimensional network, enable to entrap liquid oil easily [14]. As the wax crystals grow, they intertwine and create a physical barrier that traps the oil molecules within the network. This network can be rigid or more elastic depending on the wax type and concentration used [15]. Studies have reported that relatively low concentrations of wax, 1-4 wt%, are needed to form three-dimensional networks, enable to both adsorb oil onto the network surface, but also entangling the oil within the network pores [16]. Examples of the most common waxes used as oleogelators are carnauba wax, candelilla wax, rice bran wax and beeswax, all also being widely used in several industries, including coatings, pharmaceuticals, food products and cosmetics [13]. While natural waxes possess the capability to be utilized in oleogels, their integration often introduces challenges regarding organoleptic and sensory properties [17]. Despite their functionality in structuring oils, the incorporation of waxes can impart undesirable flavours or alter the mouthfeel of food products. Therefore, there is a preference to minimize the amount of wax in used in oleogels, to maintain the desired taste and sensory experience of the final product in regards to the food production industry.

2.2.2.2 Rice bran wax

Rice bran wax (RBW) originates from the outer layer of rice bran and is extracted during the refining process of rice bran oil, a byproduct of rice milling, hence being a byproduct and readily available in regions with substantial rice cultivation,

such as Asia. Structurally, RBW consists mainly of long-chain aliphatic wax esters and long-chain aliphatic acids, and to a lesser extent a mixture of fatty alcohols and hydrocarbons, which contributes to a relatively high melting point of the wax. Trace amounts of free fatty acids and phospholipids may also be present, [18]. Its crystalline structure consists of elongated needle-like and fibrous crystals arranged in a random orientation. These crystals form a network of interlocking structures, contributing to the semi-crystalline nature of the wax [15].

2.2.2.3 Beeswax

Beeswax (BW) is a natural secretion produced by honey bees, vital for constructing honeycomb cells, hence its production is limited by the seasonal nature of beekeeping and the decline in bee populations. Chemically, the main constituents of BW are palmitate, palmitoleate, and oleate esters of long-chain aliphatic alcohols containing 30-32 carbon atoms [18]. Its crystalline structure is characterized by long needle-like crystals packed together in a tight lattice arrangement. These crystals exhibit a highly organized structure, forming layers that stack upon each other [15].

2.2.2.4 Candelilla wax

Candelilla wax (CW) is harvested from the leaves of the candelilla shrub (Euphorbia cerifera) and is a natural plant wax extracted by boiling the leaves and stems of the shrub. The candelilla plant is native to northern Mexico and the southwestern United States, hence its availability can be influenced by environmental factors and regional harvesting regulations. Structurally, candelilla wax comprises a complex mixture of esters, hydrocarbons, and free fatty alcohols, the main component being the n-alkane hentriacontane (78.9%), with self-assembly properties in organic solvents. The crystalline structure of candelilla wax is characterized by tightly packed, needle-like crystals arranged in a mesh-like pattern. These crystals form interlocking networks, creating a dense and uniform structure [16].

2.2.2.5 Carnauba wax

Carnauba wax (CBW) originates from the leaves of the Brazilian palm tree Copernicia prunifera. Structurally, it comprises a mixture of high-molecular-weight esters of acid and hydroxy acids and its crystalline structure is characterized by large, plate-like crystals tightly packed together [19]. Although being generally regarded as safe (GRAS) and food grade, carnauba wax is most commonly used as a surface treatment material, such as for car and shoe polish [2].

2.3 Formulating oleogels

Oleogelation is known as the process of transforming liquid oils into semi-solid or solid materials called oleogels. This transformation is achieved by incorporating specific gelators into the oil phase, resulting in a three-dimensional network that immobilizes the oil and confers gel-like properties. The two main approaches for formulating oleogels are called direct dispersion and indirect dispersion, and their

use mainly depends on the chemical characteristics of the gelator, such as chain length and polarity [14].

2.3.1 Direct dispersion

Direct dispersion is known as one of the most straightforward approaches in oleogel production. Primarily, the process begins with the selection of a suitable oil, which in this case with emphasis on being used in PBMAs, would be choosing healthy, edible oils rich in unsaturated fatty acids, such as rapeseed oil. Secondly, the gelator is selected, which most commonly include LMWOGs, such as natural waxes, that are able to crystallise and form networks that entrap the oil, but HMWOG polymers that can build three-dimensional networks within the oil phase to create the desired gel structure, such as ethyl cellulose are also of interest. The main principle of the direct dispersion method is then to directly disperse the oleogelator into the continuous phase, the liquid oil, at temperatures above the gel formation temperature. The solution is then mixed using various techniques, including magnetic stirring for low-viscosity systems, ultrasonication for superior mixing efficiency, and high-shear mixing for effective homogenization. Following the mixing and cooling of the solution, the gelation process takes place. Depending on the gelling agent, this may involve cooling to induce crystallization in LMW molecules or providing resting time for polymer-based gels to develop their network via self-assembly or entanglement mechanisms. The result is a stable structure where the oil is immobilised within the gelling agent's network. Natural waxes and polymers like ethyl cellulose are commonly used oleogelators in the direct dispersion method due to their suitability to this relatively simple production process [14]. Several indirect dispersion methods can be used to form oleogels, such as biphasic emulsion or solvent exchange [2]. As they are not used in this thesis work however, they are not further described.

2.4 Rheology

Rheology is the study of the flow and deformation behaviour of materials under applied forces, encompassing both liquids and solids. It examines how materials respond to stress, strain, and deformation, providing insights into their mechanical properties, such as viscosity, elasticity, and viscoelasticity. To understand the measurements of these properties, there are several parameters to analyze, which are described hereafter.

2.4.1 Storage and loss modulus

The storage modulus (G') and loss modulus (G'') are fundamental parameters used to characterize the viscoelastic behaviour of materials like oleogels. The storage modulus, G', reflects the ability of a material to store elastic energy and resist deformation. It represents the solid-like characteristics of the material, with higher values indicating greater stiffness and structural integrity. On the contrary, the loss modulus, G'', represents the ability of a material to dissipate energy and flow.

Higher *G"* values suggest a softer, more fluid consistency, indicating liquid-like behaviour. Together, *G'* and *G"* provide insights into the mechanical properties and structural stability of oleogels. The complex shear modulus (*G**) is a combination of *G'* and *G"*, representing the overall viscoelastic response of the material. *G** offers a comprehensive understanding of the behaviour, encompassing both its solid-like and liquid-like properties [20]. The definition of the law of elasticity for oscillatory shear tests is shown in equation 2.1,

$$G^* = \frac{\tau_A}{\gamma_A} \tag{2.1}$$

with the complex shear modulus, (*G**) in pascal, is given by dividing the shear-stress amplitude τ_A (in Pa), and strain amplitude γ_A, which is dimensionless or simply expressed in % [21]. As described, (*G**) explains the entire viscoelastic behaviour of a material and can be further connected to the loss and storage moduli via a vector diagram, as shown in figure 2.2.

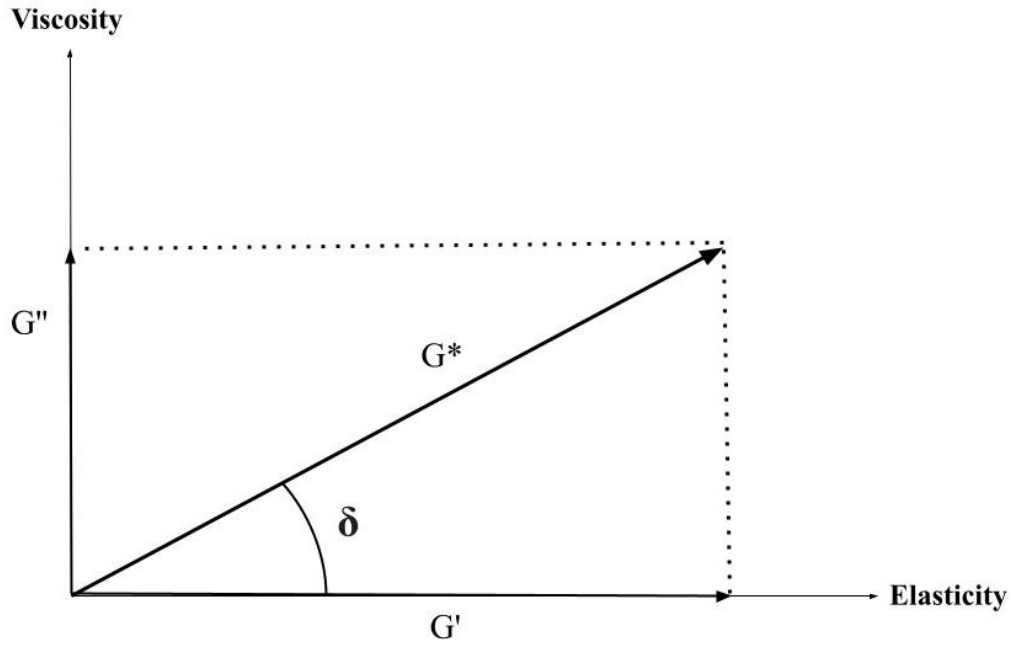

Figure 2.2: Vector diagram illustrating the relationship between storage modulus *G'* (elastic shear), *G"*(viscous shear) and complex shear modulus *G**, including the phase shift angle δ. The y-axis represents the viscous portion, while the x-axis represents the elastic portion. (Made in Google Drawings).

The tangent delta ($\tan(\delta)$), also known as the phase shift angle, is also a critical parameter used to evaluate the viscoelastic behaviour of materials such as oleogels, as it represents the ratio of the loss modulus (*G"*) to the storage modulus (*G'*). The definition of tangent delta is shown in equation 2.2,

$$tan(\delta) = \frac{G''}{G'} \tag{2.2}$$

which shows the ratio between the storage and loss moduli, offering insights into the balance between the elastic, or solid-like, behaviour and viscous, or liquid-like, behaviour of materials. A lower tan(δ) value suggests a more solid-like behaviour, indicating that the material stores more elastic energy and exhibits less flow or deformation under stress. Conversely, a higher tan(δ) value signifies a more liquid-like behaviour, where the material dissipates more energy and flows more readily [20].

To evaluate tan(δ) from rheological data, it can be connected to the phase angle, which in turn measures the phase difference between the stress and strain oscillations in the viscoelastic material [20]. Tan(δ) is directly related to the phase angle through the trigonometric relationship and follows the same pattern, hence a low phase angle also indicates more solid-like behaviour and vice versa.

2.4.2 Rheometry

Rheometery measures the viscoelastic properties with respect to time, temperature, frequency, and stress-strain. In more detail, the storage modulus *G'* and the loss modulus *G"* give measurements of the elastic and viscous behaviour of a material respectively. These measurements contribute to the characterization of the structural integrity of the oleogels, their ability to withstand external forces and deformations, and their flow properties under different conditions. Understanding the rheological behaviour of oleogels is crucial for optimising formulations, predicting their performance in processing and storage, and ensuring their suitability for specific applications such as food texture modification [22]. Significant for this thesis is the utilisation of a type of rheological technique, namely rheomicroscopy. Rheomicroscopy combines rheometry and microscopy which allows for simultaneous analysis of material properties and microstructure of the oleogels, hence making it possible to determine the underlying mechanisms for crystallisation, melting of fats and more [23].

2.4.3 Amplitude and frequency sweep

Amplitude and frequency sweep tests pose as starting measurements in rheological characterization, providing insights into the viscoelastic properties and structural dynamics of oleogels under different conditions, such as varying strain and shear stress [20].

Amplitude sweep, also known as strain sweep, involves applying a sinusoidal oscillatory shear strain at a constant frequency while measuring the resulting stress response. This test helps to determine the linear viscoelastic region (LVR), where the material's response is linear to strain amplitude. In the LVR, the storage modulus, *G'*, represents the elastic behaviour of the material, indicating its ability to store energy, while the loss modulus, *G"*, represents its viscous behaviour, reflecting energy dissipation. The crossover point, where *G'* equals *G"*, indicates the onset of non-linear viscoelastic behaviour [20]. Hence, within the LVR, the oleogels exhibit linear stress-strain relationships, indicative of their elastic and viscous properties.

However, at higher strain amplitudes, nonlinear effects such as yielding or flow behaviour may occur, providing insights into the mechanical stability and structural integrity of the oleogel network. The critical strain at which such nonlinear behaviour initiates can serve as a useful parameter for characterizing the mechanical strength of the oleogels [20].

Frequency sweep involves subjecting the sample to a sinusoidal oscillatory shear stress at varying frequencies while maintaining a constant strain amplitude. This test enables the assessment of the viscoelastic response of the material during a specific time frame, providing insights into its molecular structure and relaxation dynamics. The storage and loss moduli are frequency-dependent, with the storage modulus typically dominating at low frequencies, indicating the dominance of elastic behaviour, while the loss modulus may surpass the storage modulus at higher frequencies, signifying increased viscous behaviour [20].

2.4.4 Oscillation and rotation

In rheometry, two primary methods, oscillation, and rotation measurements, are utilized to evaluate the viscoelastic properties of materials. Oscillation measurements involve subjecting the material to an alternating stress or strain, as the input, while monitoring the strain or stress output. The same sinusoidal straining motion recurs repetitively, with each cycle under a specific time window, and having a frequency that is inversely proportional to that time, providing insights into its viscoelastic behaviour across different frequencies [20]. This technique is particularly valuable for analyzing soft materials like gels, polymers, and complex fluids. Conversely, rotation measurements apply a constant shear rate or stress that is the same in more or less everywhere of the material to observe its flow behaviour, aiding in determining viscosity, shear thinning behaviour, and flow properties [20]. This method is beneficial for assessing fluids with simpler rheological behaviour, such as liquids, pastes, and emulsions.

2.5 Differential scanning calorimetry

Differential scanning calorimetry (DSC) is a thermodynamical tool for directly assessing the uptake of heat energy, which occurs in a sample within a regulated increase or decrease in temperature. The sample is placed in an aluminium crucible, also called pan, and undergoes a precisely regulated heating or cooling ramp. Simultaneously, the DSC monitors the rate of heat flow, between the sample and a pre-selected inert reference material, such as an empty crucible. During an endothermic process, such as melting, the sample absorbs heat to maintain the temperature rise. This heat absorption is reflected in a positive deviation of the heat flux curve compared to the reference. Conversely, exothermic processes, like crystallization, release heat from the sample to maintain the temperature profile. This exothermic event is represented as a negative deflection in the heat flux curve relative to the reference. By analyzing these deviations in heat flow, the DSC quantifies the enthalpy, the heat absorbed or released, associated with thermal transitions within the

sample [24]. More specifically, it can be used to analyze the thermal properties of oils and oleogels. For oils, DSC can determine key parameters such as melting points and enthalpies, providing insights into their stability and suitability for processing. When applied to oleogels, it also aids in characterizing gelation properties, including gelation temperature and strength, as well as melting behaviour [24].

3
Methods

This section explains the methodology and materials chosen to prepare the oleogels and how their structural, thermodynamic and rheological properties were assessed and analysed.

3.1 Materials

For the preparation of oleogels, as the liquid oil phase rapeseed oil was used, named AKOPLANET RSO 100-17 and obtained from AAK (Karlshamn, Sweden). The oleogelators chosen were rice bran wax (RBW), beeswax (BW), carnauba wax (CBW) and candelilla wax (CW), obtained from TER Chemicals (Hamburg, Germany) in the form of pastilles. A fatty acid analysis was conducted by Eurofins in connection to the FOMA project at RISE, which shows the exact fatty acid content of the rapeseed oil used for this thesis, corresponding to 63.5% oleic acid, 18.6% linoleic acid and 8.7% linolenic acid, being the main contributors.

3.2 Oleogel preparation

For the production of oleogels, the direct dispersion method was utilized, and for all gels, rapeseed oil was used as the liquid oil phase, while different gelators of natural waxes were implemented as oleogelators.

3.2.1 Wax-based oleogels

Two different concentrations of wax were used, 10% w/w and 5% w/w, dispersed in rapeseed oil, 90% w/w and 95% w/w respectively. As natural waxes have been proven to form 3D networks at relatively low amounts, these two concentrations were chosen accordingly. It was also determined that having higher concentrations of waxes was not of interest, as this would increase the problematic aspects of organoleptic properties of the gels since waxes do not have a pleasant taste. Additionally, only these two concentrations were selected to reduce the number of samples needed to be tested. First, the corresponding amount of oil was weighed in a beaker. Secondly, the wax was weighed separately and then added to the beaker with oil to obtain the correct weight concentrations of the two components. The wax and oil solutions were then heated during continuous stirring, using a heating plate and magnetic stirrer, to approximately 10 °C higher than the melting temperatures of

the corresponding waxes, which can be seen in table 3.1. To ensure the dissolution of the wax pastilles, the solutions were heated to 95 °C for RBW and CBW, and to 80 °C for BW and CW. When the pastilles of wax were no longer visible, approximately 5 minutes after reaching corresponding temperatures, the solutions were poured into aluminium tins and kept at room temperature. The oleogels were stored at room temperature before being subjected to further analysis.

Table 3.1: Ranges of melting temperatures for the waxes used in the making of the oleogels according to the manufacturers TER Chemicals (Hamburg, Germany).

Wax	Melting temperature
Rice bran wax	78-84 °C
Carnauba wax	82-86 °C
Beeswax	62-65 °C
Candelilla wax	66-72 °C

Each of the constructed oleogel is shown in table 3.2, where the weight percentage of the gelator is displayed while the remaining weight is constituted of the rapeseed oil in each sample.

Table 3.2: Overview of constructed oleogels displaying the sample names, the used gelator and the weight percentage of the gelator.

Sample	Gelator	w/w%
RBW10	Rice bran wax	10
RBW5	Rice bran wax	5
BW10	Beeswax	10
BW5	Beeswax	5
CW10	Candelilla wax	10
CW5	Candelilla wax	5
CBW10	Carnauba wax	10
CBW5	Carnauba wax	5

A primary visual screening of the constructed gels was conducted by placing samples of them in corresponding glass vials, covering the bottom section of the vials. The vials were then put into a 105°C oven until the gels were completely melted, before being put on the lab bench to let cool at room temperature for 1 hour. The vials were then covered with lids and put upside down for 10 minutes to evaluate the observational liquid and fluid behaviour of the gels.

3.3 Rheological measurements

Rheological characterization of oleogels was performed using a hybrid rheometer (HR30, TA Instruments) equipped with appropriate geometries for each measurement technique and a rheomicroscope to record the microscopic changes visually. The instrument is shown in figure 3.1.

Figure 3.1: Images of the HR30, hybrid rheomicroscope, used for the rheological and microscopic measurements.

The microscope is attached below the glass plate where the samples are being placed. Above the glass plate, an upper peltier heating plate is equipped and together, this geometry enables microscopic visualisation of the samples during controlled temperature sweeps and oscillatory strain.

3.3.1 Amplitude sweep

Amplitude sweep experiments were conducted to find the linear viscoelastic region (LVR) and detect any nonlinear behaviour within the oleogel structure. During the amplitude sweeps, the rheometer applied sinusoidal stress at a fixed frequency while the strain amplitude was gradually increased from 0.01% strain to 20% strain, with a fixed gap of 200 μm. By monitoring the resulting strain response, the rheological behaviour of the oleogels under varying levels of deformation could be examined and the LVR was determined.

3.3.2 Frequency and temperature sweeps

Temperature ramp tests were performed to investigate the thermal stability and phase transitions of the oleogels over a range of temperatures. By subjecting the oleogel samples to controlled heating or cooling cycles, changes in their rheological properties were observed. For this method, an upper peltier plate system, with a fixed gap of 200 μm, to control the heating and cooling cycles, and a rheomicroscope to observe the thermal events during the cycles was used. The method involved first performing a frequency sweep, using 0.05% strain and a frequency range of 20 Hz to 1 Hz, on the sample at 25 °C, before heating it to 90 °C where it soaked for 180

seconds. The sample was then cooled, using a fixed rate of temperature change of 2 K/min, down to 5 °C. The sample was then heated to 25 °C and subjected to one more frequency sweep, before being heated with the same fixed heating rate of 2 K/min to 90 °C. The sample was then let to be cooled to 25 °C without measuring before ending the experiment.

3.3.3 Rheomicroscopy

As mentioned, the rheometer was connected to a 20X rheomicroscope during the sweeps to enable visualization of the thermal events of the oleogels at different temperatures. For this method, the focus was set on the upper peltier plate at a gap of 100 μm, while then having 200 μm during the sweeps to achieve a focus in the middle of the gels to observe the formation and melting of crystals. A brightness of 90% and polarized light was also implemented to improve the visibility of the crystals on the microscopic level.

3.4 Differential scanning calorimetry

To evaluate the thermal behaviour of the waxes, rapeseed oil and the prepared oleogels, a differential scanning calorimeter (DSC 1 STAR System, METTLER TOLEDO), equipped with nitrogen as purge gas for the cooling system, was used. The instrument was first calibrated using indium, with a known onset of 156 °C. The samples were prepared by weighing approximately 3 mg in designated 40 μm aluminium pans before being sealed. The lids of the pans were perforated with a small metal needle to let air in and out of the pans, before being placed in the instrument. Each sample was then named and the exact weight of the samples was noted in the software of the DSC. The rate of temperature change was set to 2 K/min and the method used for each sample was repeated for three replicates.

Firstly, rapeseed oil was prepared in the aluminium pans and subjected to DSC. For this method, the oil was cooled to -100 °C and then heated to 25 °C, with isothermal soaking times of 5 minutes at each endpoint. Secondly, rice bran wax, candelilla wax, beeswax and oleogels constructed with the same waxes, were subjected to the DSC method with different temperature ranges, beginning with an initial equilibration at 25 °C for 5 minutes. The samples were heated to 100 °C and maintained isothermal for 5 minutes, to then be cooled to -85 °C, maintained isothermal for 5 additional minutes. This heating and cooling cycle was repeated one more time, meaning that the samples were heated to 100°C and cooled to -85 °C, before heating the samples once more to 25 °C before finishing the experimental run. Heating and cooling rates were kept constant at 2 K/min.

All of the samples, RSO, waxes and the oleogels were also subjected to a different DSC experiment, using the same limits for temperatures, but with a rate of 2 K/min instead of 10 K/min. This was done to evaluate the effect that different heating and cooling rates have on the thermal properties of the different components, both individually and in the formed oleogels.

4

Results and discussion

This section deals with the results, firstly showing the visual screening of the prepared oleogels, moving further with the rheological measurements and lastly showing the DSC. The results are followed by an evaluation and discussion.

4.1 Oleogel preparation

The results from the first visual screening of the constructed gels show the observational differences in sol-sate of the gels, seen in figure 4.1. The sol-gel transition refers to the transformation of a solution into a gel-like network. Initially, the oleogel is in a sol state where the oil and gelling agent are homogeneously mixed, resembling a liquid or viscous solution. As the temperature decreases or other external factors change, the gelling agent starts to form a three-dimensional network within the oil phase.

Figure 4.1: Visual appearance of the oleogels with rice bran wax (RBW), beeswax (BW), carnauba wax (CBW) and candelilla wax (CW) at 10% and 5% w/w wax.

For the oleogels with 10% w/w wax, shown at the top of figure 4.1, no liquid-like behaviour was seen, as they all stayed at the top of the vials, showing higher viscosity and more solid-like properties after being cooled. Regarding the 5% w/w wax-based oleogels shown at the bottom of the image however, both the carnauba wax gel (CBW5) and rice bran wax gel (RBW5) showed more viscous and liquid-like behaviour, as CBW5 was running down the vial walls and RBW5 ended up completely on the bottom of the vial after cooling.

From the results of the visual screening, three waxes with 10 w/w% distribution were selected for further examination, RBW10, CW10 and BW10, and they are displayed in figure 4.2, taken after they have been cooled down at room temperature for 24 hours.

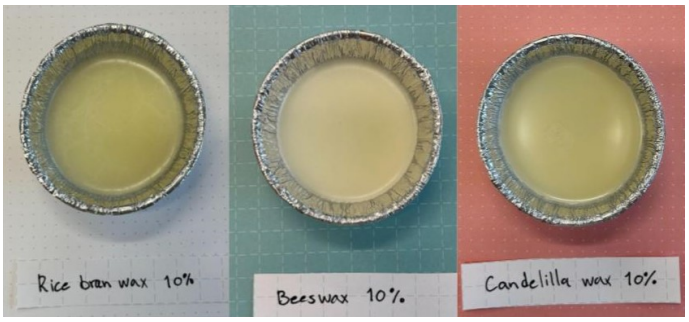

Figure 4.2: Overview of constructed olegels with 10% w/w of rice bran wax (RBW10), beeswax (BW10) and candelilla wax (CW10).

The reasoning behind choosing 10% w/w RBW, BW and CW was mainly to reduce the number of variables and gelators when advancing to further analysis. Although every wax used in this thesis work is GRAS and food grade, RBW and BW possess more direct links to food products, hence being more obvious choices to move further with. CBW and CW however are not as easily connected to food products as they are to cosmetics or industrial products, hence only CW was chosen to move further with these two, due to its interesting characteristics and lower melting point compared to CBW.

4.2 Rheological measurements

4.2.1 Amplitude sweeps and frequency sweeps

Each oleogel, RBW10, BW10 and CW10, was first subjected to an amplitude sweep to find the LVR. While it differed slightly between the different gels, it was determined to be within the region of 0.01% strain and 0.1% for all, and 0.05% strain was selected as the setting for the following frequency sweeps. The results from the amplitude sweeps are not shown, as they simply pose as an initial step in determining settings for the frequency and temperature sweeps.

The results from subjecting the three oleogels to frequency sweeps are shown in

figure 4.3 which displays the change in storage modulus and phase angle during frequency oscillations from 0.1 Hz to 20 Hz.

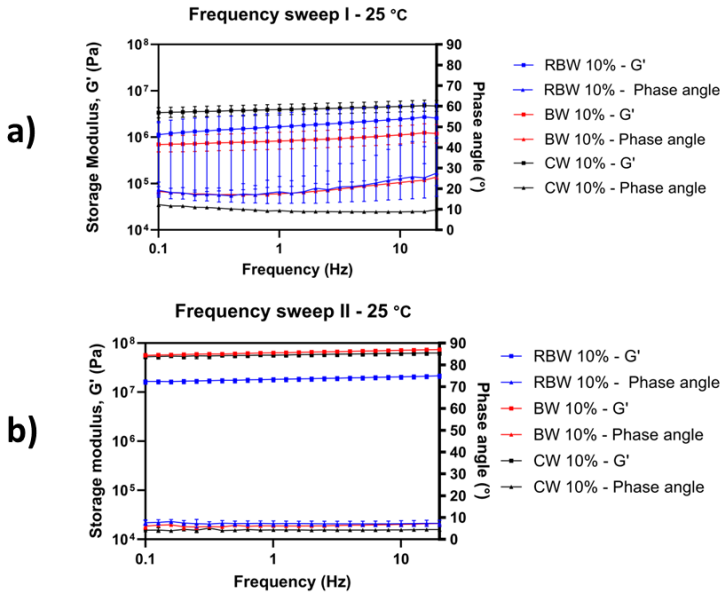

Figure 4.3: Frequency sweeps of the oleogels RBW10, BW10 and CW10. Both sweeps are at 25 °C. a) Frequency sweep I, shown at the top, refers to the sweep conducted directly after placing the oleogel on the plate. b) Frequency sweep II, in the bottom, occurs after exposing the gels to one heating and one cooling ramp.

For both graphs, the range intervals for the three replicates of each sample are shown as error bars, meaning that the error bars show the intervals of the highest and lowest replicate values, while the actual data points display the mean values from the replicates. However, as the results for the different gels varied, the error bars were more easily visible for RBW10 and BW10 than for CW10, which had fewer variations within the three replicates. Therefore, after cooling the gels during a controlled condition, the results varied far less in comparison, hence the error bars being much smaller for the second frequency sweep. The first frequency sweep conducted directly after placing the samples on the glass plate and setting the gap for the peltier plate and temperature to 25°C, resulted in relatively large variations within the sample replicates, apart from CW10. This may not only be due to not having a controlled cooling ramp before but also due to different shears when placing the samples on the plate. The second frequency sweep at 25 °C, starting after one cycle of heating and cooling of the samples, showed far fewer variations within the sample replicates. The highest values of G' were obtained for BW10, closely followed by CW10, while RBW10 showed a lower G' in comparison. In regards to the phase angle, it varied between 4°and 9°for the different gels, being in the higher range for RBW10 and the lower for CW10, indicating a predominance of elastic behaviour over viscous behaviour, with a higher storage modulus and a lower loss modulus.

As the second frequency sweep showed significantly fewer variations between the

samples, it indicates that from a controlled cooling of the oleogels, a more uniform and stable structure is formed by the waxes. Considering the crystalline structure of the waxes as the main responsible aspect of their gelation capabilities, the results from the frequency sweeps also indicate that the larger RBW crystals are less uniformly dispersed into the RSO, while BW and CW, show less variation within both frequency sweeps, creates more homogeneous and structured networks to entrap the oil. According to the literature, CW and BW create more dense networks than RBW, which might also explain that these gels have slightly higher G' for the second frequency sweep, and fewer variations within samples [15],[16]. The difference in G' could also be explained by the shear that the oleogels are being subjected to when they are applied on the plate before starting the measurement, as this could affect the stability of the gels, whereas, during the controlled cooling, they can form more stable networks. However, as it was still of interest to compare the stability and mechanical properties of the gels, before and after being subjected to a cooling ramp, it was decided to not heat the samples before placing them on the plates.

4.2.2 Temperature sweeps

The results from the temperature sweep of the gels performed in the rheometer are shown by using the data from all three replicates for each sample and then displaying only the mean values from the replicates in the graphs. In Appendix 1 however, individual graphs are shown for each oleogel, also displaying the range intervals for the three replicates. First shown in the results is the change in storage modulus (G') at different temperatures, from both the cooling and heating ramp in figure 4.4. Secondly, the phase angle is shown in figure 4.5, but shown as separate cooling and heating ramps, enabling an easier visualisation of the data.

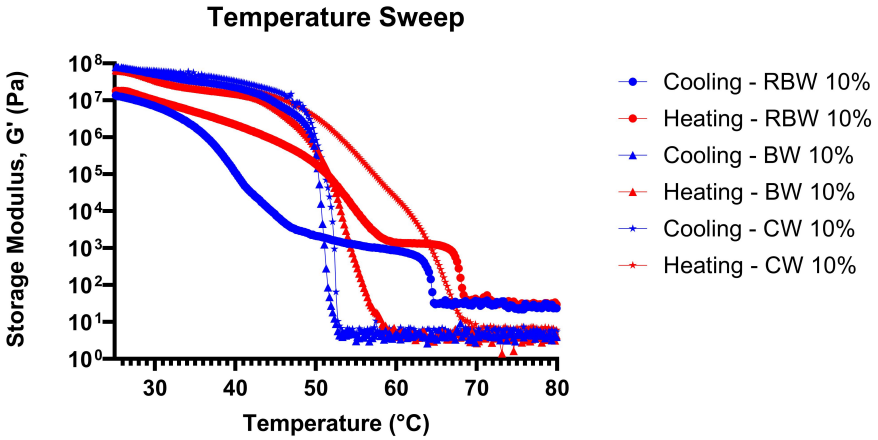

Figure 4.4: Temperature sweeps, from 80 °C to 25 °C and back, of the oleogels RBW10, BW10 and CW10. Cooling ramps are shown in blue and heating ramps in red, with different representative symbols for each oleogel.

The graph in figure 4.4 shows six different curves, corresponding to the changes in G' for one cooling and one heating ramp for the three different gels RBW10, BW10 and CW10. The cooling ramp started after heating the samples from 25 °C to 90

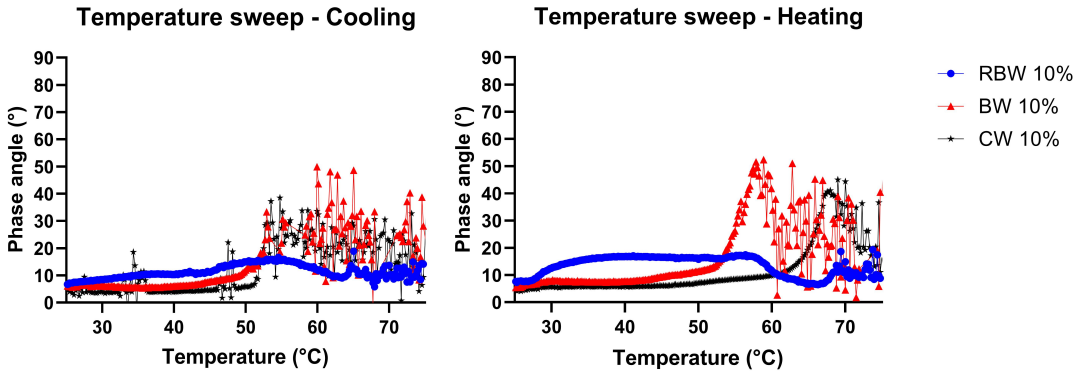

Figure 4.5: Temperature sweeps of the oleogels RBW10, BW10 and CW10 showing the response of the phase angle during cooling and heating ramp separately.

°C, hence it is followed from right to left in the graph and resulted in two very similar patterns for BW10 and CW10. Although beginning to increase at a few degrees lower for BW10, G' increased sharply between 55 °C and 50 °. For RBW10 however, G' started to increase earlier, at around 65°C but only shortly, before plateauing for a while at 1000 Pa to 50°C, and then increasing again at a slower pace until about 30 °C where the graph plateaus again. After being cooled down, a heating ramp was recorded for the gels from 25°C to 80°C. The heating ramp followed similar changes in G' for all samples, but the curves are displaced to the right, indicating that the melting of the crystals occurred at higher temperatures than the formation of the crystals. It is also notable that the changes in G' during the heating ramp were less sharp, as G' were reduced at a slower pace with increasing temperature, although eventually reaching more or less the same values for G' as for the cooling ramp. Further, it is notable to add that even though the method for the temperature sweeps, subjected the samples to a heating and cooling ranging from 5 °C to 90 °C. However, for values below 25 °C and above 80 °C, which is the interval shown in the graphs, the data points were not considered to be trustworthy, as the gels were either very stiff and solid at lower temperatures or complete liquids at higher temperatures. Hence, values of G' are not shown for these temperatures.

The graphs of the phase angles are shown in figure 4.5, which enables an evaluation of the impacts of both storage and loss modulus for the gels, as the phase angles, measured during the temperature sweeps, indicate if the responses from the gels to the oscillations are more dependent on G' or G". The phase angle is higher for RBW10 than for BW10 and CW10, indicating that RBW10 is not as solid and stiff as the other gels. However, as the phase angle is relatively low for all gels, it is clear that the majority of the response is due to a higher G' than G". After the temperature reaches values close to those corresponding melting temperatures for the wax that structures the gels, the data becomes very difficult to read, as the gels at these points are beginning to break down and becoming liquids, hence making it very complex for the plate geometry in the rheometer to give accurate responses. It is notable however, that for the heating ramp, the readings are much more stable,

even as the gels close in on the melting temperatures, as the curves increase more uniformly before the gels become too viscous for the data to be correctly interpreted. Once again, the shape of the RBW10 differs from BW10 and CW10, indicating that the chemical composition and morphology of the wax crystals structuring the gels are of the highest importance in how the gels respond during the thermal events.

4.2.3 Rheomicroscopy

During the temperature sweeps, a rheomicroscope was applied to follow the microscopic structures of the oleogels during the heating and cooling ramps. In the subsequent figures, individual temperature sweeps for each isolated oleogel are depicted. Accompanying these graphs are snapshots captured at two distinct time points: one during cooling and another during heating. These images are positioned within the graphs to highlight their respective approximate temperature points and are shown in figures 4.6, 4.7 and 4.8.

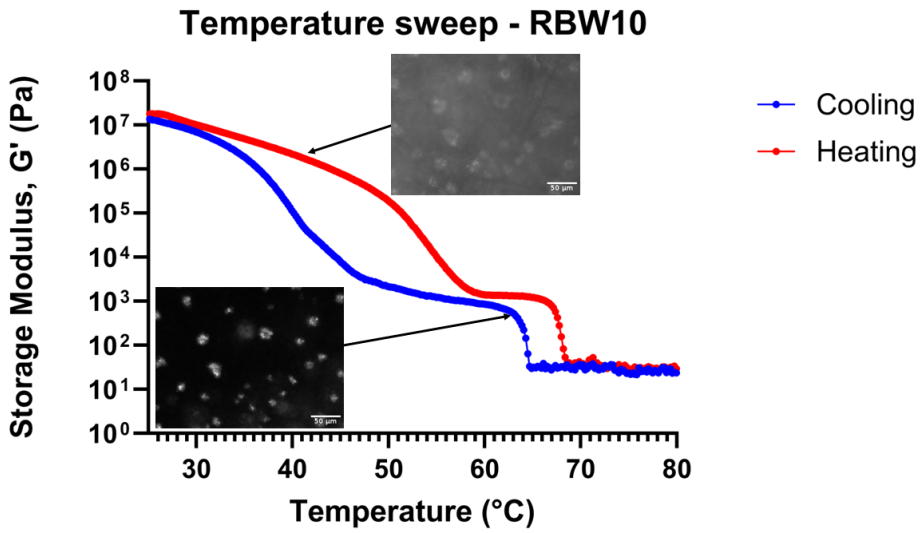

Figure 4.6: Isolated temperature sweep of RBW10 with images from the rheomicroscope at two approximate points during the cooling and heating ramps.

First shown is the temperature sweep of RBW10 in figure 4.6. The microscopic images display that the 10% w/w RBW added to the RSO forms round dendritic crystals, following a branching pattern, during the cooling ramp. The crystallisation is slower than for BW and CW but starts earlier. As mentioned, RBW primarily consists of long-chain wax esters, which contributes to the formation of a more dendritically shaped crystalline structure than a needle-like structure [10]. However, as RBW are also reported to form needle structures in other oleogel formulations, it is clear that the solvent plays a vital role in determining the crystal morphology, as the chemical components of waxes interact differently depending on the solvent [25]. It is also mentioned from previous research that the crystals from RBW form a more randomly oriented network, which fits the data from the temperature sweep of RBW shown in Appendix 1. During the cooling ramps for the three replicates,

the values for G' differ relatively broadly for RBW in comparison to BW and CW, which in turn creates more structured networks [15],[16]. The randomly oriented and dendritic crystals of RBW also explain the weak sol-gel state of RBW5, previously discussed from visual screening in figure 4.1.

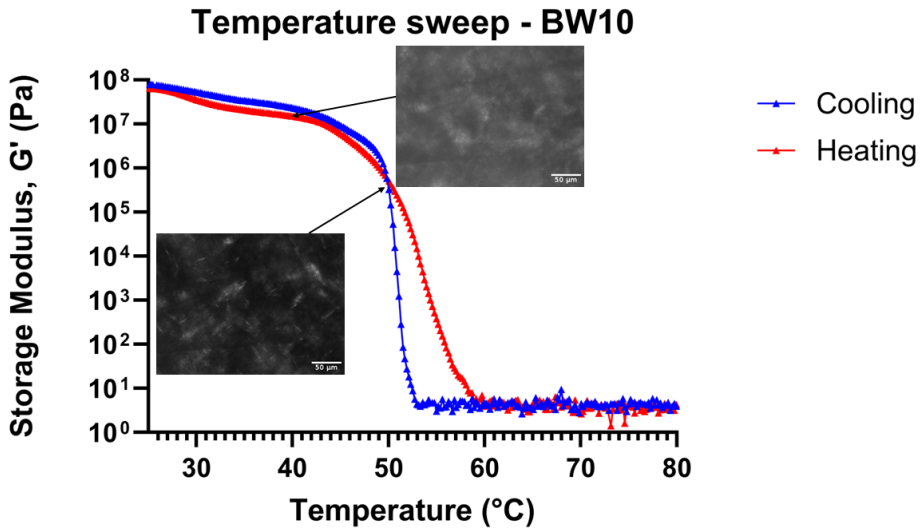

Figure 4.7: Isolated temperature sweep of BW10 with images from the rheomicroscope at two approximate points during the cooling and heating ramps.

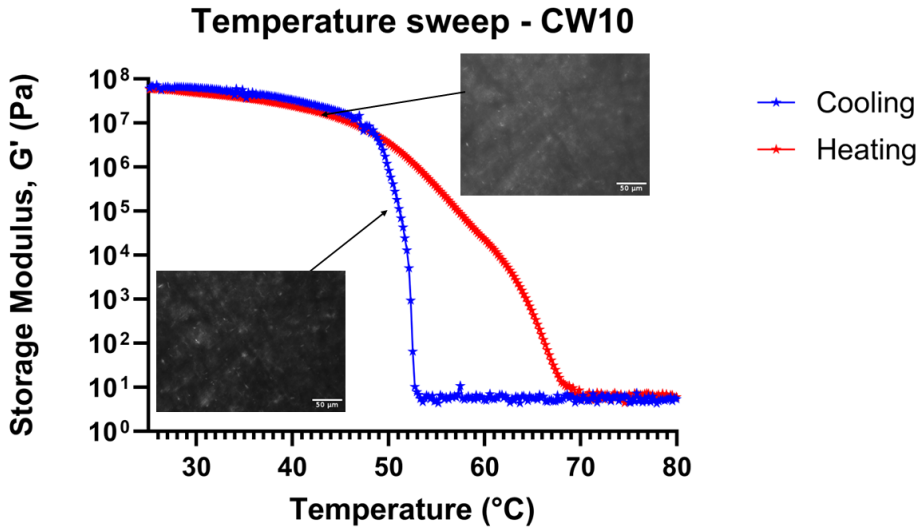

Figure 4.8: Isolated temperature sweep of CW10 with images from the rheomicroscope at two approximate points during the cooling and heating ramps.

Secondly, the temperature sweep of BW10 is shown in figure 4.7 and lastly, the temperature sweep of CW10 is shown in figure 4.8. The structure of BW and CW

are much more alike and fit well with literature indicating that both waxes form needle-like and dense structures [15],[16]. The cooling ramps show, as previously mentioned, sharp changes in G' while the heating ramp changes less rapidly. For CW, the heating ramp shows the slowest changes in G', which potentially is due to the smaller and denser crystalline structure of CW, also being the reason behind the higher melting temperature for CW than that for BW.

An approximate point of crystallisation from the microscopy is shown for all three oleogels in figure 4.9, displaying the formation of crystals. The images visualise more clearly that RBW forms round dendritically shaped crystals while BW and CW form needle-like crystals. By comparing BW and CW more thoroughly, one might also assume that the CW crystals are smaller and larger in number than BW. However, it is difficult to determine from these images alone.

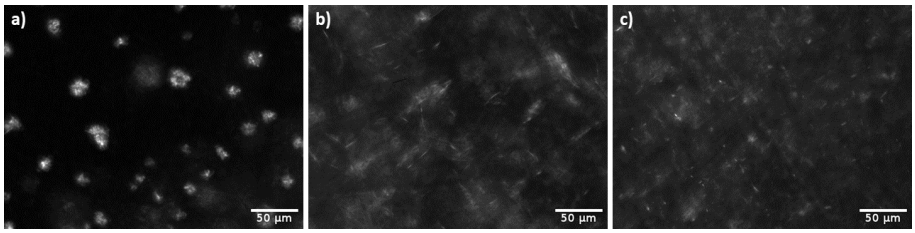

Figure 4.9: Snapshot images from the cooling ramps of the temperature sweep, at the time points when crystallisation is visible, a) RBW10, b) BW10 and c) CW10.

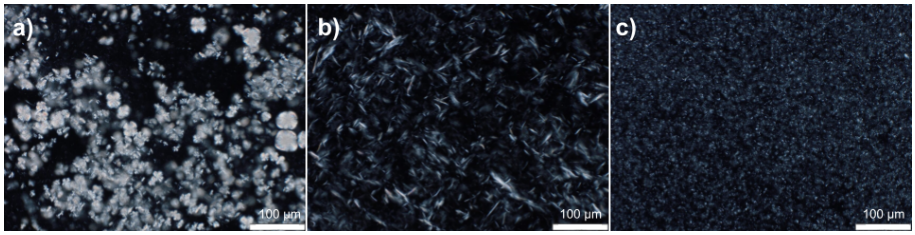

Figure 4.10: Polarised light microscopy images of a) RBW10, b) BW10 and c) CW10.

To confirm the imaging of the crystalline structures from the rheomicroscopy, RBW10, BW10 and CW10 were also subjected to polarised light microscopy. In another master's thesis in FOMA, dealing with diffusion concerning the microscopic structure of the gels, light microscopy images were kindly contributed to this thesis work to complement the rheomicroscopy images. The light microscopy images are shown in figure 4.10. The images are taken using a 20X objective, the same as for rheomicroscopy, but as the images are taken from two different instruments the scales are not the same, as the field of view and other variables differ. Polarised light microscopy visualises the crystals more clearly than the images from rheomicroscopy, but they both show the same structures for the different formulations. Thus, it was confirmed that RBW forms larger and rounder crystals, while BW and CW form thin, needle-like crystals. CW forms the most dense structure as the crystals are very small in relation to BW and RBW. Once again, this can be connected to the

chemical composition of the waxes, mentioned in the theoretic background of the oleogelators.

4.3 Thermal characterization

The results from DSC are shown in separate graphs for rapeseed oil, waxes and lastly the combined oleogels, respectively. One standard curve of each sample is displayed in the graphs, while mean values and standard deviations for onset temperature, peak temperature and integrated normalised changes in enthalpy, are shown in the corresponding tables. Exothermic reactions are displayed as positive changes in the graph, while endothermic correspond to negative enthalpy changes, hence the cooling ramps will show positive values and the heating ramps will show negative values of heat flow.

4.3.1 Rapeseed oil

Firstly, rapeseed oil was subjected to DSC resulting in the graph shown in figure 4.11. The mean and standard deviation values for onset and peak temperatures, as well as enthalpy changes, are compiled in table 4.1.

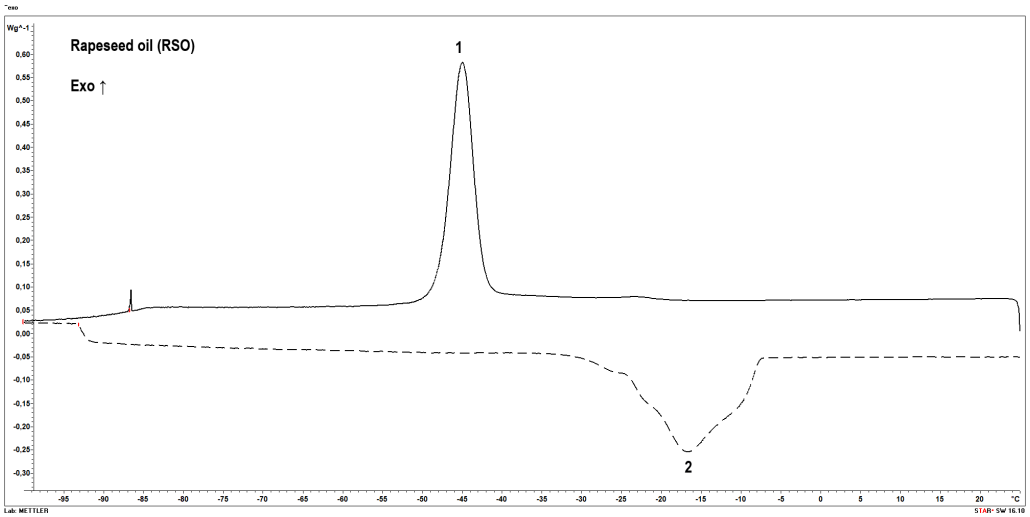

Figure 4.11: DSC of rapeseed oil (RSO).

Table 4.1: Calculated mean and standard deviation values for the three replicates of rapeseed oil (RSO) from DSC.

	T1			**T2**		
Sample	**Onset °C**	**Peak °C**	**△H J/g**	**Onset °C**	**Peak °C**	**△H J/g**
RSO	-42.4±0.3	-44.8±0.2	53.5±0.2	-25.1±0.9	-16.7 ±0.1	-69.9±0.8

The graph displays an exothermic peak at around -45 °C corresponding to a heat flow out of the aluminium pan of 53.5 J/g. During the heating ramp, an endothermic peak appears at around -20 °C corresponding to heat flow into the aluminium pan of -69.9 J/g. Hence, the formation of the crystals for RSO occurs at lower temperatures than for the melting of the crystals. This could be due to a phenomenon called supercooling, where a material is kept in its liquid state at a temperature lower than its solidification temperature [26]. When a liquid crosses its standard freezing point, it will crystallize if a seed crystal or nucleus is present, around which a crystal structure can form, resulting in a solid. In the absence of such nuclei, the liquid phase can be maintained down to the temperature at which homogeneous nucleation of crystals occurs [26].

4.3.2 Waxes

The results from DSC on waxes are shown in figure 4.12 while the data is compiled in table 4.2. The image shows two areas of peaks. The peaks at T3 correspond to exothermic processes as the waxes are being cooled and thus forming crystals at the corresponding peak and onset temperatures, laying very close to each other, indicating a very rapid solidification. For the peaks at T4 however, the onset temperature starts earlier and is followed by distinct peaks at approximately 78 °C for RBW, 63 °C for BW and 66 °for CW. The changes in enthalpy range from 148 J/g to 188 J/g for the exothermic peaks, being highest for RBW and lowest for CW. For the endothermic peaks, the enthalpy changes range from -181.6 J/g for RBW and 180.4 J/g for BW, to -153.5 J/g for CW. In regards to the literature values of melting temperatures for the waxes shown in table 3.1, the peak values from the DSC all lay within the lower areas of the temperature ranges from the literature.

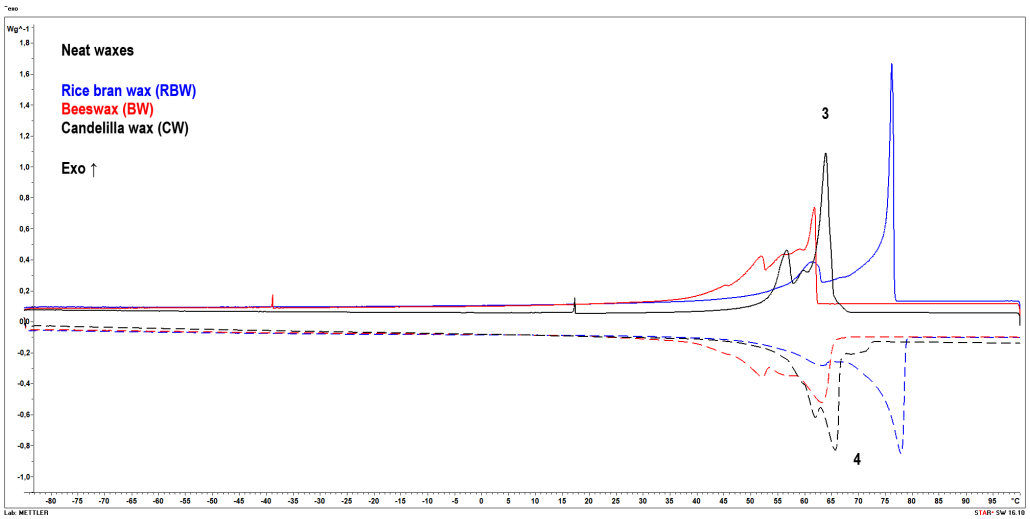

Figure 4.12: DSC of the natural waxes.

Table 4.2: Calculated mean and standard deviation values for the three replicates of the natural waxes in neat form, from DSC.

	T3			T4		
Sample	**Onset °C**	**Peak °C**	**△H J/g**	**Onset °C**	**Peak °C**	**△H J/g**
RBW	76.6±0.1	76.3±0.1	187.7±0.1	72.7±0.4	78.0±0.1	-181.6±0.7
BW	62.3±0.1	61.8±0.1	175.4±1.3	53.6±0.1	63.1±0.1	-180.4±0.7
CW	65.1±0.1	63.9±0.1	148.5±0.3	60.2±0.1	65.7±0.1	-153.5±1.0

4.3.3 Oleogels

The DSC results from the oleogels are shown in figure 4.13, while the data is compiled in table 4.3 Two endothermic and exothermic peaks appear, represented by T1 and T3 for the endothermic and T2 and T4 for the exothermic.

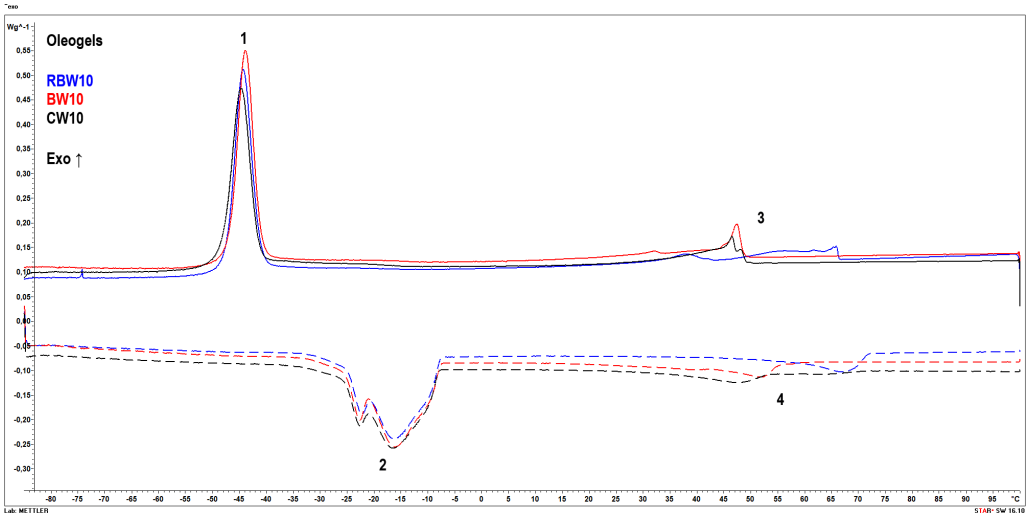

Figure 4.13: DSC of the oleogels with 10% w/w of rice bran wax (RBW10), beeswax (BW10) and candelilla wax (CW10).

Table 4.3: Calculated mean and standard deviation values for the three replicates of the oleolges with rice bran wax (RBW10), beeswax (BW10) and candelilla wax(CW10), respectively, from DSC.

	T1			T2		
Sample	**Onset °C**	**Peak °C**	**△H J/g**	**Onset °C**	**Peak °C**	**△H J/g**
RBW10	-41.2±0.1	-44.2±0.1	50.0±1.3	-23.4±0.3	-16.2±0.1	-61.5±1.2
BW10	-41.1±0.1	-43.9±0.1	49.0±0.3	-23.1±0.1	-16.1±0.1	-62.2±0.5
CW10	-41.5±0.1	-44.7±0.1	51.6±1.1	-24.3±0.3	-16.5±0.1	-60.8±0.9
	T3			**T4**		
Sample	**Onset °C**	**Peak °C**	**△H J/g**	**Onset °C**	**Peak °C**	**△H J/g**
RBW10	67.4±0.3	66.5±0.7	15.8±0.8	52.3±9.8	67.3±0.3	-17.6±1.8
BW10	49.0±0.4	47.6±0.4	14.6±0.2	41.7±0.4	51.6±0.3	-15.0±0.4
CW10	49.0±1.2	46.9±1.8	13.4±0.5	33.6±4.6	47.6±0.3	-14.5±0.6

At T1 and T2, the peaks correspond to those of RSO, also visible in figure 4.11. The shapes of the curves for the oleogels differ however slightly in comparison to the peaks of RSO. While onset and peak temperatures remain relatively similar, it seems to require slightly less energy to either crystallise or melt the structures when adding waxes to RSO and forming gels. The shape of the endothermic peak is also different for the oleogels, as there is a clearer smaller peak within the bigger peak. In regards to the peaks at T3 and T4, they correspond to the peaks of waxes also visible in figure 4.12. However, as there is much less wax than oil in the oleogels, the peaks are far less distinct and do not involve as many changes in enthalpy as when there were waxes in the aluminium pans. Moreover, there are also larger variations, considering the standard deviation values for the oleogels, indicating that the gels are not homogeneous systems and different samples may differ in amounts of wax, as the total samples are very small (around 3 mg). The largest deviations were observed for RBW10 and CW10, as the onset temperature at peak T4 differed with ±9.8 °C for RBW10 and ±4.6 for CW10. This might also be due to differences in the amount of wax in different areas of the oloegels, as the samples for the DSC are very small in comparison to the batch of the gels.

To also evaluate the impact of employing different rates of temperature change on the oleogels thermal behaviour, the gels were also subjected to DSC using a heating and cooling rate of 10 K/min instead of 2 K/min. The results are shown in figure 4.14 and 4.15. The DSC thermograms in these figures revealed sharper and narrower peaks at the slower rate (2 K/min) compared to the faster rate (10 K/min). This suggests that the slower rate allowed the oleogel crystals more time to equilibrate during the thermal transitions, leading to a more defined response.

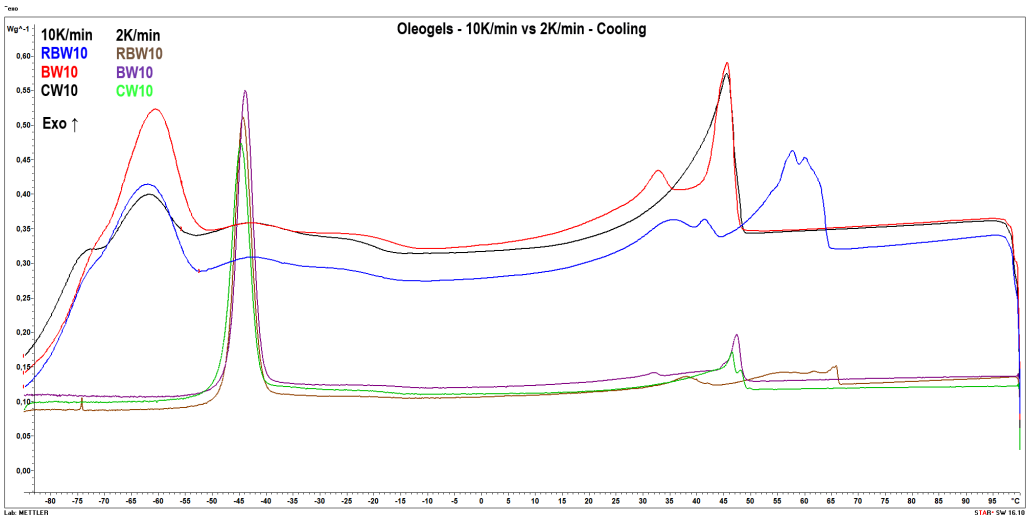

Figure 4.14: DSC showing the cooling ramp, using both 2 K/min and 10 K/min temperature change rate, of the oleogels with 10% w/w of rice bran wax (RBW10), beeswax (BW10) and candelilla wax (CW10)

To evaluate the DSC results further, they can, much like the rheological measure-

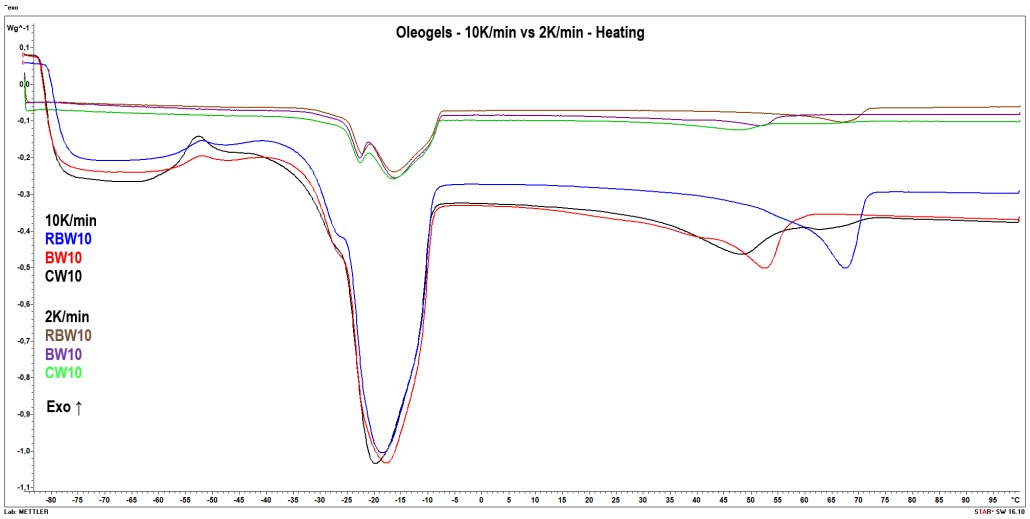

Figure 4.15: DSC showing the heating ramp, using both 2 K/min and 10 K/min temperature change rate, of the oleogels with 10% w/w of rice bran wax (RBW10), beeswax (BW10) and candelilla wax (CW10)

ments, be connected to the chemical composition of the components in the gels as well as previous research. One study that conducted several DSC experiments on RSO using cooling and heating rates of 0.5-10 K/min, showed very similar results to the DSC measurements on RSO in this thesis work [27]. This study also suggests that when using a higher cooling rate, more peaks appear on the thermograms, which also aligns with the thermograms obtained in this thesis, using first a cooling rate of 2 K/min and then a cooling rate of 10 K/min. For the higher rate of cooling, several differently shaped peaks appear in comparison to the lower cooling rate, see figure 4.14. This suggests that a higher cooling rate, forces the formation of multiple crystal structures, while for a lower cooling rate, the crystals have more time to form, hence resulting in a more uniform structure.

When evaluating the DSC results of the waxes and comparing them to the results of oleogel formulations, there are similarities. CW seems to require the least amount of energy to melt crystals and releases less energy when forming crystals, in comparison to RBW and BW. This result follows when having CW as a component in the oloegel CW10, as the forming and melting of this crystalline structure releases and requires slightly less energy than for RBW10 and BW10, as shown from T3 and T4 in table 4.3. However, the differences in enthalpy changes are not as significantly different in the oleogels as for the waxes, which is reasonable due to the low amount of waxes incorporated in the oloegels. As for the chemical composition of the waxes, the results from DSC indicate that the intramolecular forces in RBW are stronger than those in BW and CW, even though the crystalline structures seem to be more uniform and organised for BW and CW. This is most likely due to the higher amount of long-chain wax esters in RBW, while BW and CW consist more of fatty alcohols and hydrocarbons [16],[18].

4.4 Methodological evaluation

4.4.1 Choice of oleogels

From the beginning of this thesis work, it was determined to focus on wax-based oleogels and to choose only one selection of oil as the liquid phase and four different waxes as oleogelators. This choice was mainly supported due to the ease of constructing oleogels with waxes, as they can be directly dispersed into the oil phase. However, different waxes possess different structural and thermal properties, hence the reason why to initially start with four different waxes to gain insight into how they differ from each other. Thus, the first oleogels that were made consisted of rapeseed oil and rice bran wax (RBW), beeswax (BW), carnauba wax (CBW) or candelilla wax (CW) at two different concentrations (w/w), 10% and 5% respectively. RBW, BW and CW were further evaluated thermally and structurally, and while more data were obtained in these areas, it is still difficult to recognise what exact chemical properties of the oleogelators contribute to the differences amongst the oleogels. However, it is clear from the results that the chemical structure of the oleogelator affects the gelation process and thermal behaviour during temperature ramps. It would be of importance to evaluate the same oleogelators used in this thesis work in gels with other oils than only RSO, as it has been shown that the fatty acid composition of the liquid oil phase also affects the gelation process and network formation [9], [10].

Apart from being functional components in an oleogel, sustainable and economical aspects need to be taken into account. As previously mentioned in the theoretical section of waxes, RBW is a byproduct of rice bran oil production, while BW and CW are directly harvested from their sources [15]. This presents a particularly interesting option using RBW for oleogel formulation, as this attribute not only enhances its cost-effectiveness but also aligns with sustainable production practices by utilising a material that might otherwise be discarded. Hence, leveraging RBW supports the principles of circular economy, reducing waste and adding value to the rice milling industry.

When further analysing the oleogels, it became an issue of how long the gels were stored before being subjected to measurements, as the analysis was conducted at different time points during the project. There is research indicating an ageing phenomenon of oleogels, especially those with waxes, that can affect the crystalline structure, which can change over time, leading to recrystallisation, which could impact properties like texture and firmness [28]. In this thesis work, the wax-based oleogels were made in the early stages of the experimental phase, in singlicates, and then used in the following analytical methods. This might lead to uncertainties in the obtained results of the wax-based oleogels. However, as the direct dispersion method of constructing these oleogels is very simple and is not accompanied by risks for errors, it was determined it was not needed to make replicates of the oleogels. For the potential ageing effect, the samples were first subjected to a heating ramp in both the DSC and rheometry measurements and then cooled, with a conditioning

cooling rate to control the formation of recrystallization, hence deleting the thermal memory of the primary crystalline structure as well as errors or inaccurate results following the potential ageing effect.

In the early stages of developing the oleogels, it was determined to also exploit and prepare gels with a different gelator, namely the polymer ethylcellulose (EC). The positive aspect of also including this would be that a different gelator than natural waxes would be implemented and analysed in comparison to the wax-based gels and that EC gels are also possible to construct using direct dispersion. However, implementing EC gels in the project would also create yet another variable to take into account, and to complete direct dispersion of EC in RSO needs temperatures at 145-150 °C. Repeated heating could potentially reduce these PUFAs and MUFAs, and increases less desirable saturated fats, posing a health risk of the created oleogel if implemented in food products [29]. Heating can also create unhealthy compounds like free radicals and trans fats, although the amount in rapeseed oil is likely to be lower than some other oils [29].

4.4.2 Rheology

Considering the techniques and methods used for the rheological measurements, it was chosen to develop a method focusing on producing stable data during the gelation phase of the gels, as well as the stability of the gels after the formation of crystals. As mentioned, the method started with a frequency sweep, followed by a heating ramp. This resulted in data showing first the variation within the samples from the first frequency sweep, and then producing data with far less sample variation as the thermal memory of the gels was deleted from the heating ramp. The data points from the rheometry were relatively stable before reaching temperatures above the melting points of the corresponding waxes, this method worked well for the evaluation of the gelation and the stability and firmness of the crystalline networks. However, it could also be interesting to evaluate the gels during higher temperatures, enabling a comparison to the cooking of PBMAs, and lower temperatures, similar to storage temperatures of frozen PBMAs. It would although be very difficult to evaluate the oleogels in this thesis at higher temperatures, as the crystalline networks collapse at these temperatures and result in a liquid solution of dissolved wax in oil. Even if a different plate geometry were implemented, such as a cross-hatched plate to increase the friction between the plate and the gels, it would still be very difficult to measure, as the response would be mostly from the loss modulus, G". At frozen storage temperatures, around -20 °C, the gels would instead be very stiff and firm, also making the measurements more complex. Therefore, in this thesis work, it was determined to focus on achieving good measurements within the temperature range before and during the gelation process.

A heating and cooling rate of 2 K/min was chosen, mostly because a higher rate would induce a risk of less uniform heating and cooling from the plate and pushing on the boundaries that the used rheometer would produce accurate results. It would be of higher interest to use a lower cooling rate, as the results from DSC strongly

suggest that the rate of cooling affects the crystal formation. It was determined however, as this would increase the run time of the experiments and add one more variable to the rheological measurements, that only one rate of temperature change would be used, and that the focus would be on comparing the different gelators used rather than anything else.

In regards to the rheomicroscopy imaging used to evaluate the crystal structure further, it was both suitable and easily applicable to complement the data from the temperature sweeps. However, it would have been more favourable to implement some form of sophisticated image analysis of the images, to evaluate the sizes and density of crystals formed and enhance the quality of the images taken during the formation and melting of crystals. As this demands significantly more time, it was determined to simply extract the images from the rheometer, but it would be interesting to process and evaluate the images further. As a complementary tool however, the combination of rheometry and rheomicroscopy allowed for a more comprehensive investigation of the relationship between the microstructure, crystalline behaviour and resulting rheological properties of the oleogels, thereby acting as an initial guiding of further optimization of formulation parameters for specific applications in food.

4.4.3 DSC

In regards to the DSC methodology, it was firstly determined to use the same cooling and heating rate as for the rheological measurements, which enabled a direct comparison between the results obtained from the corresponding technique used. This procedure also began with a heating ramp to delete the thermal memory in the oleogels, reducing variation between samples as they were all measured during the same conditions. As the DSC machine was automated and experiments could be run during nights without attending the machine, there was also time to subject the samples to one other rate of temperature change, namely 10 K/min, which is the standard rate used in the area of DSC. When comparing the different cooling and heating rates, narrower peaks were obtained with the slower cooling and heating rate (2 K/min) suggesting a more gradual and controlled phase transition, allowing for sufficient time for molecular rearrangements and crystallization processes to occur. This finer resolution may indicate the presence of multiple crystalline phases or polymorphic forms within the oleogel matrix, which could influence its mechanical properties, stability, and functionality. Conversely, the broader peak observed with the faster cooling and heating rate (10 K/min) implies a more rapid and less controlled phase transition, potentially leading to incomplete crystallization or phase segregation within the oleogel structure. Therefore, by analysing two different cooling and heating rates, opened up another area of research in regards to the formation of the crystalline structure, both in RSO and in waxes.

The DSC method used on RSO ranged from -100 °C to 25 °C, as it was within this

interval the most interesting phase transitions were anticipated to occur. For waxes, the DSC was run to -85 °C, which was not necessary as it was known beforehand that the crystallisation occurred in the ranges of 40 to 80 °C. Hence, the procedure could have been conducted within the ranges above negative temperatures to save time. However, it could be of importance to also evaluate the long-term behaviour of the oleogels in lower temperatures, to compare it to the storage of PBMAs, containing oleogels, in freezers for example.

The thermograms achieved from DSC were directly evaluated and extracted from the DSC software. This made the x- and y-axis somewhat difficult to see and the curves were not as efficiently displayed as they could be by extracting the data from the DSC software and using a separate software to construct graphs. However, the graphs displayed in this thesis work still show the most important shapes of the curves and peaks relatively clearly when the RSO waxes and oleogels are displayed separately.

5

Conclusion and prospects

The natural waxes, including RBW, BW, CW, and CBW, demonstrated effective oleogelation properties when combined with rapeseed oil at concentrations of both 5 and 10% w/w wax. Despite exhibiting higher viscosity at 5% concentration, all waxes successfully formed gels with rapeseed oil. CW and BW effectively entrapped the oil phase at both concentrations, while RBW resulted in a less firm gel at 5% but solidifying at 10%.

The method for rheomicroscopy was successfully implemented, allowing simultaneous analysis of oleogels at both rheological and microscopic levels. The chemical composition of the waxes played a crucial role in their interaction with the liquid oil phase and the formation of the gel network. CW and BW exhibited dense, organised needle-like crystal structures that effectively entrapped the oil phase, while RBW formed round dendritic crystals with a more random distribution. Oleogels containing CW and BW displayed organized crystal structures with minimal variation among triplicate samples, whereas RBW-formed crystals exhibited more variability. RBW oleogels demonstrated stability at higher temperatures due to their melting point around 80°C. In turn, DSC confirmed phase transitions of both waxes and oleogel components, aligning well with previous research findings. Additionally, DSC analysis revealed significant variations in crystallisation behaviour with different temperature change rates, suggesting that a slower cooling rate enables the crystals to form in a more structured manner, requiring less energy, highlighting the influence of thermal kinetics on crystalline structure formation.

Looking ahead, future research in the field of oleogels holds promising avenues for exploration and innovation. Incorporating additional components into oleogel formulations, such as lecithin and fibres derived from citrus and peas, presents intriguing possibilities for enhancing structural integrity and functionality while potentially reducing the amount of wax required. Lecithin, known for its emulsifying properties, can contribute to improved stability and texture of the oleogels, which have been proven in previous studies [30], while citrus and pea fibres offer the potential to enhance gel network strength and provide nutritional benefits [31]. Moreover, there is a pressing need for further investigation into the application of oleogels in plant-based meat analogues, particularly in terms of their behaviour during processing techniques like extrusion. Understanding how oleogels withstand extrusion and other manufacturing processes is crucial for optimising their performance and sensory attributes in plant-based meat products. By focusing future research efforts on these areas, the full potential of oleogels in the food industry can be unlocked.

Bibliography

[1] Deepinder Kaur, Dina A. Tallman, and Pramod Khosla. The health effects of saturated fats – the role of whole foods and dietary patterns. *Diabetes & Metabolic Syndrome: Clinical Research & Reviews*, 14(2):151–153, 3 2020.

[2] Shaziya Manzoor, F. A. Masoodi, Farah Naqash, and Rubiya Rashid. Oleogels: Promising alternatives to solid fats for food applications. *Food Hydrocolloids for Health*, 2:100058, 12 2022.

[3] Ibrahim M Dighriri, Abdalaziz M Alsubaie, Fatimah M Hakami, Dalal M Hamithi, Maryam M Alshekh, Fatimah A Khobrani, Fatimah E Dalak, Alanoud A Hakami, Efham H Alsueaadi, Laila S Alsaawi, Saad F Alshammari, Abdullah S Alqahtani, Ibrahim A Alawi, Amal A Aljuaid, and Mohammed Q Tawhari. Effects of Omega-3 Polyunsaturated Fatty Acids on Brain Functions: A Systematic Review. *Cureus*, 10 2022.

[4] Zoran Petrovic, Vesna Djordjevic, Dragan Milicevic, Ivan Nastasijevic, and Nenad Parunovic. Meat Production and Consumption: Environmental Consequences. *Procedia Food Science*, 5:235–238, 2015.

[5] Christina Kendler, Arvid Duchardt, Heike P. Karbstein, and M. Azad Emin. Effect of oil content and oil addition point on the extrusion processing of wheat gluten-based meat analogues. *Foods*, 10(4), 4 2021.

[6] Katsuyoshi Nishinari. Some thoughts on the definition of a gel. *Progress in Colloid and Polymer Science*, 136:87–94, 2009.

[7] Madline Schubert, Nelli Erlenbusch, Sebastian Wittland, Sharline Nikolay, Birgit Hetzer, and Bertrand Matthäus. Rapeseed Oil Based Oleogels for the Improvement of the Fatty Acid Profile Using Cookies as an Example. *European Journal of Lipid Science and Technology*, 124(11), 11 2022.

[8] Chloe M. O'Sullivan, Shai Barbut, and Alejandro G. Marangoni. Edible oleogels for the oral delivery of lipid soluble molecules: Composition and structural design considerations. *Trends in Food Science & Technology*, 57:59–73, 11 2016.

[9] Angela Borriello, Nicoletta Antonella Miele, Paolo Masi, Alessandra Aiello, and Silvana Cavella. Effect of fatty acid composition of vegetable oils on crystallization and gelation kinetics of oleogels based on natural wax. *Food Chemistry*, 375:131805, 5 2022.

[10] Iris Tavernier, Chi Diem Doan, Davy Van De Walle, Sabine Danthine, Tom Rimaux, and Koen Dewettinck. Sequential crystallization of high and low melting waxes to improve oil structuring in wax-based oleogels. *RSC Advances*, 7(20):12113–12125, 2017.

[11] Jim H.C. Lee, Sendhil K. Poornachary, Xin Yi Tee, Liangfeng Guo, Connie K. Liu, Liling Zhang, Tiedong Sun, Qiubo Chen, Jianwei Zheng, and Pui Shan

Chow. Effect of Base Oil Polarity on the Functional Mechanism of a Viscosity Modifier: Unraveling the Conundrum of Coil Expansion Model. *Industrial and Engineering Chemistry Research*, 62(48):20567–20578, 12 2023.

[12] R.J. Mailer. Oilseeds, Overview. *Reference Module in Food Science*, 1 2016.

[13] Chi Diem Doan, Iris Tavernier, Paula Kiyomi Okuro, and Koen Dewettinck. Internal and external factors affecting the crystallization, gelation and applicability of wax-based oleogels in food industry. *Innovative Food Science & Emerging Technologies*, 45:42–52, 2 2018.

[14] Tzyi Horng Tan, Eng Seng Chan, Maslia Manja, Teck Kim Tang, Eng Tong Phuah, and Yee Ying Lee. Production, health implications and applications of oleogels as fat replacer in food system: A review, 9 2023.

[15] Alexia I. Blake, Edmund D. Co, and Alejandro G. Marangoni. Structure and physical properties of plant wax crystal networks and their relationship to oil binding capacity. *JAOCS, Journal of the American Oil Chemists' Society*, 91(6):885–903, 2014.

[16] J. F. Toro-Vazquez, J. A. Morales-Rueda, E. Dibildox-Alvarado, M. Charó-Alonso, M. Alonzo-Macias, and M. M. González-Chávez. Thermal and textural properties of organogels developed by candelilla wax in safflower oil. *JAOCS, Journal of the American Oil Chemists' Society*, 84(11):989–1000, 11 2007.

[17] Till Wettlaufer. *Wax-based Oleogels-from Fundamentals to Food Applications vorgelegt von Zusammenfassung In einer Vielzahl von Lebensmitteln werden Fette mit einem hohen Anteil an gesättigten.* PhD thesis, Technical University of Berlin, Berlin, 2022.

[18] Sarbojeet Jana and Silvana Martini. Physical characterization of crystalline networks formed by binary blends of waxes in soybean oil. *Food Research International*, 89:245–253, 11 2016.

[19] Bo Ra Yi, Mi Ja Kim, Su Yong Lee, and Jae Hwan Lee. Physicochemical properties and oxidative stability of oleogels made of carnauba wax with canola oil or beeswax with grapeseed oil. *Food Science and Biotechnology*, 26(1):79–87, 2 2017.

[20] Howard A. Barnes. *A handbook of elementary rheology.* University of Wales, Institute of Non-Newtonian Fluid Mechanics, 2000.

[21] Thomas Mezger. Applied Rheology with Joe Flow on Rheology Road. *Anton Paar GmbH*, 2014.

[22] Jian Zhao, Xiangrui Xi, Hang Dong, Zhihua Wang, and Zewen Zhuo. Rheo-microscopy in situ synchronous measurement of shearing thinning behaviors of waxy crude oil. *Fuel*, 323:124427, 9 2022.

[23] Qiang Wang, Aimin Shi, and Faisal Shah. Rheology instruments for food quality evaluation. *Evaluation Technologies for Food Quality*, pages 465–490, 1 2019.

[24] Pooria Gill, Tahereh Tohidi Moghadam, and Bijan Ranjbar. Differential Scanning Calorimetry Techniques: Applications in Biology and Nanoscience. Technical report, National Library of Medicine, 2010.

[25] Sorina Ropciuc, Florina Dranca, Mircea Adrian Oroian, Ana Leahu, Ancuţa Elena Prisacaru, Mariana Spinei, and Georgiana Gabriela Codină. Characterization of Beeswax and Rice Bran Wax Oleogels Based on Different Types

of Vegetable Oils and Their Impact on Wheat Flour Dough Technological Behavior during Bun Making. *Gels*, 10(3), 3 2024.

[26] I. Shamseddine, F. Pennec, P. Biwole, and F. Fardoun. Supercooling of phase change materials: A review. *Renewable and Sustainable Energy Reviews*, 158:112172, 4 2022.

[27] Yayoi Miyagawa and Shuji Adachi. Analysis of nonisothermal crystallization of rapeseed oil by deconvolution of differential scanning calorimetry curve. *Journal of Oleo Science*, 68(12):1215–1222, 2019.

[28] Dafni Dimakopoulou-Papazoglou, Foteini Giannakaki, and Eugenios Katsanidis. Structural and Physical Characteristics of Mixed-Component Oleogels: Natural Wax and Monoglyceride Interactions in Different Edible Oils. *Gels*, 9(8), 8 2023.

[29] Ayesha Baig, Muhammad Zubair, Sajjad Hussain Sumrra, Muhammad Faizan Nazar, Muhammad Nadeem Zafar, Kausar Jabeen, Muhammad Bilal Hassan, and Umer Rashid. Heating effect on quality characteristics of mixed canola cooking oils. *BMC Chemistry*, 16(1), 12 2022.

[30] Paula K. Okuro, Iris Tavernier, Mohd D. Bin Sintang, Andre G. Skirtach, António A. Vicente, Koen Dewettinck, and Rosiane L. Cunha. Synergistic interactions between lecithin and fruit wax in oleogel formation. *Food and Function*, 9(3):1755–1767, 3 2018.

[31] Pui Yeu Phoon and Christiani Jeyakumar Henry. Fibre-based oleogels: effect of the structure of insoluble fibre on its physical properties. *Food and Function*, 11(2):1349–1361, 2 2020.

A

Appendix 1

A.1 Temperature sweeps

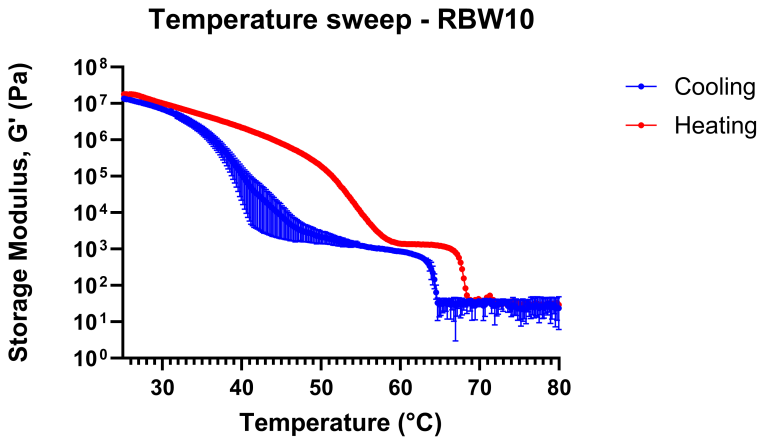

Figure A.1: Isolated temperature sweep of RBW10 with error bars showing the range intervals of the three replicates.

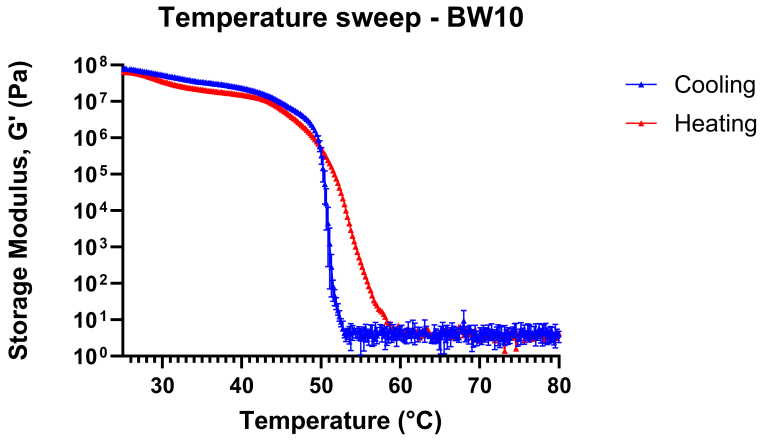

Figure A.2: Isolated temperature sweep of BW10 with error bars showing the range intervals of the three replicates.

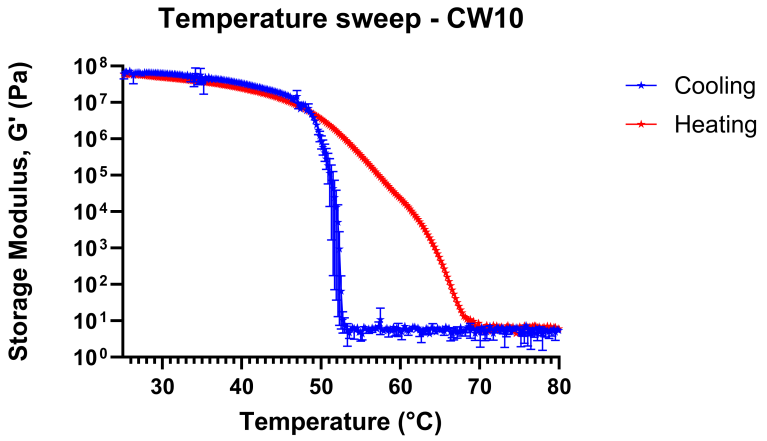

Figure A.3: Isolated temperature sweep of CW10 with error bars showing the range intervals of the three replicates.

The graphs above, shown in figures A.1, A.2 and A.3, display the individual temperature sweeps of the oleogels RBW10, BW10 and CW10. The data points are showing the mean value of three replicate for each gel, but also displaying error bars, corresponding to the range interval of the highest and lowest value from the replicates.

DEPARTMENT OF CHEMISTRY
CHALMERS UNIVERSITY OF TECHNOLOGY
Gothenburg, Sweden
www.chalmers.se

CHALMERS
UNIVERSITY OF TECHNOLOGY